International Journal of Heat and Mass Transfer 117 (2018) 846–860

Contents lists available at ScienceDirect

International Journal of Heat and Mass Transfer

journal homepage: www.elsevier.com/locate/ijhmt

Conductive heat transfer in rarefied binary gas mixtures confined between parallel plates based on kinetic modeling

Christos Tantos, Dimitris Valougeorgis *

Department of Mechanical Engineering, University of Thessaly, Volos 38334, Greece

ARTICLE INFO

Article history:
Received 21 July 2017
Received in revised form 7 October 2017
Accepted 8 October 2017

Keywords:
Kinetic theory
Rarefied gas dynamics
Binary gas mixtures
Kosuge model
Transport coefficients
Intermolecular models
Micro heat transfer

ABSTRACT

The kinetic model introduced by Kosuge (2009) is implemented to solve heat transfer through rarefied binary gas mixtures confined between two parallel plates maintained at different temperatures. The results have been found to be in very good agreement with corresponding ones obtained by the Boltzmann equation, the DSMC method and the Chapman-Enskog analysis. The efficiency of the Kosuge model for this problem is clearly demonstrated in the whole range of the Knudsen number for various heat flow setups, even when the temperature difference between the plates is large. The following three intermolecular models have been implemented: Hard Sphere (HS), Lennard Jones (LJ), Realistic Potential (RP). The computed HS heat fluxes in the transition and viscous regimes vary significantly with the corresponding ones of the LJ and RP models, which are close to each other. Also, the intermolecular model has a significant effect on the distribution of the mole fraction between the plates, while it has a minor effect on the density and temperature distributions. Concerning the partial heat flux distributions of the light and heavy species it has been found that moving from the hot towards the cold plate the former one is decreasing, while the latter one is increasing with the total heat flux being always constant. Heat fluxes with partial thermal accommodation at the walls are reported for He-Ne and He-Xe. For the same mixtures dimensional heat fluxes in terms of the reference pressure are plotted indicating that the total heat fluxes of the mixture with various mole fractions are always bounded from below and above by the heat flux of the heavy and light species respectively. These data may be useful for comparisons with experiments. Applying the equivalent single gas approach, it is deduced that this concept is not useful in rarefied binary gas mixture heat flow problems, which should be treated by two coupled kinetic equations. Finally, the effective thermal conductivity approximation has been successfully applied, provided that the system Knudsen number remains adequately small.

1. Introduction

The steady-state conductive heat transfer through rarefied gases confined between solid surfaces is a classical problem and, in the case of monatomic single gases, has been extensively investigated. The available research work includes heat transfer between parallel plates [1–4], coaxial cylinders [5–9] and concentric spheres [10–14] under small and large temperature differences. Since the solution of the Boltzmann equation is computationally very demanding, most of the research is based on the numerical solution of the Bhatnagar-Gross-Krook (BGK) [15], Ellipsoidal (ES) [16] and Shakhov (S) [17] kinetic models [18]. In [3,6,7,9,10–12] small values of the temperature difference between the surfaces are considered and the computed heat fluxes are obtained solving the linearized form of the corresponding kinetic model equations, while in [1,4,5,8,13,14] large temperature differences are maintained between the walls and the results are based on the nonlinear form of the model equations. In all cases, provided that the thermal conductivity coefficient is properly recovered, reliable results have been reported in the whole range of the Knudsen number. The Direct Simulation Monte Carlo (DSMC) method [19] has been also implemented to simulate this classical problem and to test various molecular interaction models [20] as well as to validate new approaches and numerical methods [21–24]. In addition, based on the Holway [16] and Rykov [25] models, as well as on the DSMC method, the problem of heat conduction through polyatomic gases has been recently tackled pointing out the effect of the rotational and vibrational degrees of freedom of the molecules [26–28]. In addition, unsteady heat conduction through monatomic and polyatomic rarefied gases in plane

* Corresponding author.
E-mail address: diva@mie.uth.gr (D. Valougeorgis).

https://doi.org/10.1016/j.ijheatmasstransfer.2017.10.050
0017-9310/

and cylindrical geometries caused by a sudden change of the wall temperature has been considered in [29–31].

The corresponding research work in the case of gas mixtures, although in practice gaseous mixtures are used more frequently than single gases, is not as extensive. In the case of small temperature differences the McCormack model [32] has been proven to be a reliable model [33–36], properly recovering simultaneously all transport coefficients and it has been applied to simulate steady [36,37] and transient [38] heat flow between plates. Recently, a detailed evaluation of the McCormack model is presented in [39] by comparing its solutions for the Couette and Fourier flows of binary gas mixtures with corresponding results of the linearized Boltzmann equation. Furthermore, the McCormack model allows the implementation of any type of intermolecular model and as reported in [36] the computed heat fluxes, particularly near the hydrodynamic regime, strongly depend on the molecular interaction law. In the case of large temperature differences however, as far as the authors are aware off, corresponding work based on kinetic models is not available in the literature. The nonlinear heat transfer through binary gas mixtures has been solved by the Boltzmann equation with the assumption of hard sphere molecules [40] and by the DSMC method supplemented by the Ab-initio potential [41], while the transient behavior has been analyzed via the DSMC method in [42]. The required computational effort in both methodologies, particularly under the assumption of general intermolecular models, is very large and it is rather evident that the search for a kinetic model simulating the specific problem with modest computational effort, allowing in parallel an in depth investigation of all involved parameters, will be very useful.

A relatively large number of binary gas mixture kinetic models, has been proposed in the literature. As the most typical and commonly applied ones, the models of Gross and Krook [43], Sirovich [44], Hamel [45], Holway [46], Ogushi [47], McCormack [32], Garzo, Santos and Brey [48] and Andries, Aoki and Perthame [49], as well as the more recent model of Kosuge [50], which is of particular interest in the present work, are cited. All above models, except the ones by McCormack and Kosuge, suffer one or both of the following two important constrains [50,51]: (a) the parameters introduced in the molecular interactions cannot be accordingly adjusted to correctly produce all transport coefficients and (b) they are suitable only for the pseudo Maxwell molecules.

The McCormack kinetic model [32], as pointed above, circumvents both pitfalls, but it is a linear model and it is restricted to conditions close to local equilibrium. The recently introduced Kosuge model [50] has been derived, following the same polynomial expansion approach in the molecular velocity space as in the McCormack model, which now however, is applied into the nonlinear (instead of the linearized) collision term of the Boltzmann equation. The expansion coefficients are determined by the equivalence of moment method (Grad's 13-moment approximation). The resulting model equations are not restricted to pseudo Maxwell molecules and can fit to various molecular models (hard sphere, Lennard-Jones, realistic, etc.), while the transport coefficients obtained by the Chapman-Enskog analysis coincide with those of the Boltzmann equation at the first or second approximation. More precisely, the thermal conductivity, the viscosity, and the thermal diffusion coefficients coincide at the first approximation, while the diffusion coefficient up to the second approximation. Furthermore, its linearization yields the third order McCormack model [50], while there is no proof that the model (in its nonlinear form) fulfills the H-theorem.

The model has been applied in [50] for half-space and two-surface problems of a vapor in the presence of a non-condensable gas reproducing well the corresponding solutions of the Boltzmann equation. However, it has been also found that it does not work well in strongly nonequilibrium flow and this is contributed to the positivity of the velocity distribution function which is not always assured. In spite this deficiency it is recommended as an effective tool for the investigation of gas mixtures [50]. It is noted that in the Shakhov model for single gases the positivity of the velocity distribution function is also not assured but the model has been effectively applied in many rarefied flow and heat transfer setups [52–56].

Based on the above it is evident that further investigation of the validity of the Kosuge model in simulating rarefied gas dynamics problems is important. Within this framework, in the present work, the conductive heat flow through various binary gas mixtures confined between two parallel plates is computationally investigated. All macroscopic quantities (number densities, temperatures and heat fluxes) of practical interest are calculated in a wide range for all involved parameters (gas rarefaction, mole fraction, molecular mass ratio, temperature difference, etc.). A systematic comparison between the present results obtained by the Kosuge model and the corresponding ones obtained by the Boltzmann equation [40] and the DSMC method [41] is performed. The model validation is supplemented by comparing the computed thermal conductivity and thermal diffusion ratio coefficients with the ones obtained by the Chapman-Enskog theory [57]. The influence of various intermolecular potentials on the computed quantities is examined. The work is extended to partial thermal gas-surface accommodation and its effect on the computed heat fluxes is presented. The validity of the equivalent single gas approach [58] is analyzed in terms of the binary gas mixture composition and its mole fraction in a wide range of gas rarefaction. Furthermore, the effective thermal conductivity approximation, which has been successfully applied in single monatomic [21] and polyatomic [28] gases, is introduced here in the case of nobble gas mixtures.

2. Formulation of the heat transfer problem

Consider a stationary rarefied mixture of two monatomic gases, say components 1 and 2, confined between two infinite parallel plates, fixed at $\hat{y} = 0$ and $\hat{y} = L$, which are maintained at constant temperatures T_H and T_C respectively, with $T_H > T_C$. Then, due to the temperature difference, a steady one-dimensional heat flow is established in the direction normal to the plates and directed from the hot towards the cold plate. It is noted that indexes 1 and 2 always refer to the light and heavy species respectively. The objective is to investigate the validity of the Kosuge kinetic model in solving this heat flow problem and then, examine the steady behavior of the mixture in terms of (a) the mixture composition, (b) the mole fraction of the mixture, (c) the temperature difference between the plates, (d) the degree of gas rarefaction, (e) the intermolecular potential model and (f) the thermal accommodation coefficients (not necessarily in that order).

The temperature difference is introduced in dimensionless form as

$$\beta = \frac{T_H - T_C}{2T_0}, \tag{1}$$

where $T_0 = (T_H + T_C)/2$. The temperature ratio in terms of β is given by $T_H/T_C = (1+\beta)/(1-\beta)$. The degree of gas rarefaction is determined by the reference Knudsen number defined as

$$Kn_0 = \frac{l_0}{L}, \tag{2}$$

where $l_0 = [\sqrt{2}\pi d_1^2 n_0]^{-1}$ is the reference mean free path and corresponds to the mean free path of the molecules of species 1, having diameter d_1, when the gas mixture is in the equilibrium state at rest, with number density determined as

$$n_0 = n_{1,0} + n_{2,0} = \frac{1}{L}\int_0^L n(\hat{y})d\hat{y}. \tag{3}$$

The chemical composition of the mixture is characterized by its mole fraction

$$C = \frac{n_1}{n}, \tag{4}$$

where n_1 is the number density of species 1, while $n = n_1 + n_2$ is the total number density of the mixture, with n_2 denoting the number density of species 2. It is noted that the temperature difference causes a variation of the mole fraction $C = C(\hat{y})$ between the plates around its equilibrium value at T_0, defined as $C_0 = n_{1,0}/n_0$.

The state of gas mixture is determined by the set of two one-particle velocity distribution functions $f_\alpha(\boldsymbol{r}, \boldsymbol{\xi})$ $(\alpha = 1, 2)$ that depend on the space vector $\boldsymbol{r} = (x, y, z)$ and the molecular translational velocity $\boldsymbol{\xi} = (\xi_x, \xi_y, \xi_z)$. The distribution functions $f_\alpha(\boldsymbol{r}, \boldsymbol{\xi})$ obey the Boltzmann equation for gas mixtures, substituting however, the complicated collision term with the kinetic model proposed by Kosuge [50]. For the present steady-state heat transfer configuration the Kosuge kinetic equations for the one-particle distribution functions f_α is written as [50]

$$\boldsymbol{\xi}\frac{\partial f_\alpha}{\partial \boldsymbol{r}} = \sum_{\beta=1}^{2}\left\{\Phi_{\beta\alpha}\left[\frac{m_\alpha}{2\pi kT}\right]^{3/2}\exp\left[-\frac{m_\alpha \xi^2}{2kT}\right] - K_{\beta\alpha}n_\beta f_\alpha\right\}, \tag{5}$$

where $\Phi_{\beta\alpha}$ is a polynomial in ξ given by

$$\Phi_{\beta\alpha} = K_{\beta\alpha}n_\beta n_\alpha + \sqrt{\frac{2m_\alpha}{kT}}\xi_i\Phi^{(1)}_{\beta\alpha,i} + \left(\frac{m_\alpha}{2kT}\xi^2 - \frac{3}{2}\right)\Phi^{(2)}_{\beta\alpha} + \frac{m_\alpha}{2kT}\xi_i\xi_j\Phi^{(3)}_{\beta\alpha,ij} + \frac{4}{5}\sqrt{\frac{m_\alpha}{2kT}}\xi_i\left(\frac{m_\alpha}{2kT}\xi^2 - \frac{5}{2}\right)\Phi^{(4)}_{\beta\alpha,i}, \qquad \alpha = 1,2, \qquad i = x,y,z. \tag{6}$$

Here m_α is the molecular mass of species α, k is the Boltzmann constant, T is the total temperature of the mixture and $K_{\beta\alpha}$ $(= K_{\alpha\beta})$ are positive constants. As it is often used in literature [33,59] the parameters $K_{\beta\alpha}$ are appearing only in the form of $K_\alpha (= K_{2\alpha}n_2 + K_{1\alpha}n_1)$ which are defined as

$$K_1 = \frac{S_1S_2 - n_1n_2v^{(4)}_{21}v^{(4)}_{12}}{S_2 + n_2v^{(4)}_{21}}, \quad K_2 = K_1\frac{S_2 + n_2v^{(4)}_{21}}{S_1 + n_1v^{(4)}_{12}}, \quad S_1 = n_1(v^{(3)}_{11} - v^{(4)}_{11}) + n_2v^{(3)}_{21}, \quad S_2 = n_2(v^{(3)}_{22} - v^{(4)}_{22}) + n_1v^{(3)}_{12}, \tag{7}$$

where $v^{(\kappa)}_{\beta\alpha}$ are the collision frequencies given in Eq. (A.2) in [50] and they are written in terms of the macroscopic quantities and the Chapman-Cowling Ω integrals for various intermolecular potentials, which are provided in [60]. The expressions of $\Phi^{(1)}_{\beta\alpha,i}$, $\Phi^{(2)}_{\beta\alpha}$, $\Phi^{(3)}_{\beta\alpha,ij}$, $\Phi^{(4)}_{\beta\alpha,i}$ appearing in Eq. (6) are complicated expressions, also given in the Appendix A in [49]. It is noted that the expressions of $\Phi^{(1)}_{\beta\alpha,i}, \Phi^{(2)}_{\beta\alpha}, \Phi^{(3)}_{\beta\alpha,ij}, \Phi^{(4)}_{\beta\alpha,i}$ have been obtained so that the right hand of Eq. (5) and the original collision term in the Boltzmann Equation for the Grad 13-moment approximation to the velocity distribution function yield the same moments.

The macroscopic quantities of the number density n_α, partial pressure P_α, temperature T_α, normal stress tensor components $P_{\alpha ii}$ and heat flow vector Q_α in the $\hat{y}-$ direction of species α are calculated as the moments of the unknown distribution functions according to

$$n_\alpha = \int_{-\infty}^{\infty} f_\alpha d\xi, \quad P_\alpha = n_\alpha kT_\alpha = \frac{m_\alpha}{3}\int_{-\infty}^{\infty}\xi^2 f_\alpha d\xi, \quad P_{\alpha ii} = m_\alpha\int_{-\infty}^{\infty}\xi_i^2 f_\alpha d\xi, \quad Q_\alpha = \frac{m_\alpha}{2}\int_{-\infty}^{\infty}\xi_i\xi^2 f_\alpha d\xi \tag{8}$$

with $\xi^2 = \xi_x^2 + \xi_y^2 + \xi_z^2$ and $d\xi = d\xi_x d\xi_y d\xi_z$. The overall mixture quantities of number density n, pressure P and heat flow Q are calculated as the sum of the corresponding macroscopic quantities of the mixture components, while the overall temperature of the mixture is given by $T = CT_1 + (1 - C)T_2$.

For the specific problem under consideration the computational effort can be reduced by eliminating, based on the well-known projection procedure, the ξ_x and ξ_z components of the molecular velocity by introducing the reduced distributions

$$h_\alpha = \int_{-\infty}^{\infty}\int_{-\infty}^{\infty} f_\alpha d\xi_x d\xi_z, \quad g_\alpha = \int_{-\infty}^{\infty}\int_{-\infty}^{\infty} f_\alpha(\xi_x^2 + \xi_z^2)d\xi_x d\xi_z. \tag{9}$$

Furthermore, it is convenient to introduce the following dimensionless quantities:

$$H_\alpha = \frac{h_\alpha \upsilon_0}{n_0}, \quad G_\alpha = \frac{g_\alpha}{\upsilon_0 n_0}, \quad \boldsymbol{c} = \frac{\boldsymbol{\xi}}{\upsilon_0}, \quad y = \frac{\hat{y}}{L}, \quad \rho_\alpha = \frac{n_\alpha}{n_0}, \quad \tau_\alpha = \frac{T_\alpha}{T_0}, \quad p_{\alpha ii} = \frac{P_{\alpha ii}}{n_0 kT_0}, \quad q_\alpha = \frac{Q_\alpha}{n_0 kT_0\upsilon_0} \tag{10}$$

Here $\upsilon_0 = \sqrt{kT_0/m_0}$ is a characteristic speed of the mixture and $m_0 = C_0m_1 + (1 - C_0)m_2$ is the mean molecular mass with m_1 and m_2 being the molecular masses of the two species.

Operating accordingly, with the integral operators defined by expressions (9) on Eq. (5) and introducing the dimensionless quantities (10) yields the following system of kinetic equations:

$$c_y\frac{\partial H_\alpha}{\partial y} = \frac{1}{Kn_0}\left[\exp\left(-\frac{m_\alpha c_y^2}{2m_0\tau}\right)\sqrt{\frac{m_\alpha}{m_1}}\frac{L_\alpha}{\pi^{3/2}} - \frac{\sqrt{m_0}}{\pi\sqrt{2m_1}}R_\alpha H_\alpha\right], \qquad \alpha = 1,2 \tag{11a}$$

$$c_y\frac{\partial G_\alpha}{\partial y} = \frac{1}{Kn_0}\left[\exp\left(-\frac{m_\alpha c_y^2}{2m_0\tau}\right)\frac{Z_\alpha}{\pi^{3/2}} - \frac{\sqrt{m_0}}{\pi\sqrt{2m_1}}R_\alpha G_\alpha\right], \qquad \alpha = 1,2 \tag{11b}$$

Here H_α and G_α are the unknown reduced distribution functions of species α, while the expressions of L_α, Z_α and R_α are shown in Appendix A. The same non-dimensionalization and projection procedures are applied to the moments (8), to find that the macroscopic quantities in terms of H_α and G_α given according to

$$\rho_\alpha = \int_{-\infty}^{\infty} H_\alpha dc_y, \quad \tau_\alpha = \frac{m_\alpha}{3m_0\rho_\alpha}\int_{-\infty}^{\infty}\left[c_y^2H_\alpha + G_\alpha\right]dc_y, \quad \tau = C\tau_1 + (1 - C)\tau_2, \quad p_{xyy} = \frac{m_\alpha}{m_0}\int_{-\infty}^{\infty} c_y^2H_\alpha dc_y,$$
$$p_{xxx} = p_{xzz} = \frac{3\rho_\alpha\tau_\alpha - p_{xyy}}{2}, \quad q_\alpha = \frac{m_\alpha}{2m_0}\int_{-\infty}^{\infty} c_y\left[c_y^2H_\alpha + G_\alpha\right]dc_y, \quad q = q_1 + q_2 \tag{12}$$

It is noted that the energy conservation equation $\partial q/\partial y = 0$ is readily reduced which implies that the total heat flux remains constant along $0 \leqslant y \leqslant 1$ and it is implemented to benchmark the computations. However, the heat fluxes of the species vary between the plates.

To close the problem the formulation of the boundary conditions at $y = 0$ and $y = 1$ is provided. The reflected distributions at the two plates have the following form [61]:

$$f_\alpha^{(+)} = n_{w\alpha}\left(\frac{m_\alpha}{2\pi kT_\alpha^*}\right)^{3/2}\exp\left(-\frac{m_\alpha\xi^2}{kT_\alpha^*}\right), \qquad \alpha = 1,2. \tag{13}$$

The superscript $(+)$ denotes outgoing distributions and $n_{w\alpha}$ is a parameter specified for each species α by the no penetration condition at the walls. The parameters T_α^* are calculated from the energy balance equations of each species at the surface according to [62,27]

$$T_\alpha^* = a_\alpha T_w + (1-a_\alpha)\frac{E_\alpha^-}{2N_\alpha^-}, \tag{14}$$

where T_w is either the hot $(y=0)$ or cold $(y=1)$ temperatures of the plates and $a_\alpha \in [0,1]$ is the thermal accommodation coefficient of species α. Typical values of the thermal accommodation coefficient for single gases can be found in [62,63]. In Eq. (14), E_α^- and N_α^- are the incident energy and particle fluxes of species α at the walls respectively and they are both part of the solution.

Introducing in Eqs. (13) and (14), the same normalization and projection processes as for the kinetic equations, lead to the reflected reduced distributions at the boundaries given by

$$H_\alpha^{(+)} = \rho_{w,\alpha}\sqrt{\frac{m_\alpha}{2\pi m_0 \tau_\alpha^*}}\exp\left(-\frac{m_\alpha c_y^2}{2m_0\tau_\alpha^*}\right),$$
$$G_\alpha^{(+)} = \rho_{w,\alpha}\sqrt{\frac{2\tau_\alpha^* m_0}{\pi m_\alpha}}\exp\left(-\frac{m_\alpha c_y^2}{2m_0\tau_\alpha^*}\right), \tag{15}$$

where the parameters $\rho_{w,\alpha}$ are computed as

$$\rho_{w,\alpha} = \sqrt{\frac{2\pi m_\alpha}{\tau_\alpha^* m_0}}\int_0^\infty H_\alpha^{(-)} c_y dc_y, \tag{16}$$

with the superscripts $(+)$ and $(-)$ denoting outgoing and impinging distributions. The parameters $\tau_\alpha^* = T_\alpha^*/T_0$ are calculated as

$$\tau_\alpha^* = a_\alpha \tau_w + (1-a_\alpha)\frac{m_\alpha \int_0^\infty \left(c_y^2 H^{(-)} + G^{(-)}\right) c_y dc_y}{4m_0 \int_0^\infty H^{(-)} c_y dc_y}. \tag{17}$$

Also, $\tau_w = T_w/T_0$ and in terms of the temperature ratio β, $\tau_w(0) = 1+\beta$ (hot wall) and $\tau_w(1) = 1-\beta$ (cold wall).

In the present work the kinetic model Eqs. (11) with the associated moments (12) and boundary conditions (15)–(17) are solved numerically in a deterministic manner. The discretization is based on the discrete velocity method in the molecular velocity space and on a second order control volume approach in the physical space. The macroscopic quantities are computed by Gauss-Legendre quadrature. The implemented algorithm is parallel in the velocity space and has been also applied in previous works to solve with considerable success heat transfer configurations [5,26–28]. The iteration process between the kinetic equations and the corresponding moments of the distribution functions is terminated when the convergence criteria

$$\frac{1}{6K}\sum_{\alpha=1}^{2}\sum_{i=1}^{K}\left[\left|\rho_{\alpha,i}-\rho_{\alpha,i}^{pr}\right| + \left|\tau_{\alpha,i}-\tau_{\alpha,i}^{pr}\right| + \left|q_{\alpha,i}-q_{\alpha,i}^{pr}\right|\right] < \varepsilon \tag{18}$$

with the *pr* superscript denoting the corresponding quantities in the previous iteration and K the total number of nodes in the physical space, is fulfilled. The kinetic results presented in the next section have been obtained by dividing the physical space $y \in [0,1]$ into 6000 equal segments and by taking 96 discrete molecular velocities in each direction, which are the roots of the corresponding Legendre polynomial accordingly mapped from $[-1,1]$ to $[0,\infty)$. The convergence parameter is set to $\varepsilon = 10^{-6}$. These numerical parameters assure grid independent results up to the reported significant figures.

3. Results and discussion

The results are organized as follows: In Section 3.1 comparisons between the present results obtained by the Kosuge model and corresponding ones obtained by the Boltzmann equation, the DSMC method and the Chapman-Enskog theory are performed. In Section 3.2 the dependency of the macroscopic quantities on the temperature ratio T_H/T_C and the reference Knudsen number Kn_0 is investigated for several binary gas mixtures with various reference mole fractions C_0. The hard sphere (HS), Lennard-Jones (LJ) and Realistic Potential (RP) molecular models are introduced. Also, partial thermal accommodation of the components of the gas mixture at the walls is considered. Finally, in Section 3.3 the concepts of the equivalent single gas approach and the effective thermal conductivity are studied. The investigation includes virtual and noble gas mixtures. The molecular masses of the involved noble gases are: $m_{He} = 4.0026$ gr/mol, $m_{Ne} = 20.180$ gr/mol, $m_{Ar} = 39.948$ gr/mol and $m_{Xe} = 131.293$ gr/mol.

3.1. Validation of the Kosuge model

To validate the Kosuge model for the specific problem under consideration, a systematic comparison between the present results and the corresponding ones obtained by the Boltzmann equation [40], the DSMC method [41] and the Chapman-Enskog solutions [57] is performed. The comparison covers a wide range of the temperature ratio T_H/T_C, the reference mole fraction $C_0 \in [0,1]$ and the reference Knudsen number $Kn_0[0,\infty)$.

In Table 1, the dimensionless total heat fluxes q obtained by the Boltzmann equation for two virtual HS gas mixtures with $T_H/T_C = 2$ $(\beta = 1/3)$ in [40] are compared with the corresponding ones obtained here by the Kosuge model. The two mixtures have the following molecular diameter and mass ratios: $(m_2/m_1, d_2/d_1) = (2,1)$ and $(4,2)$. The gas mixture species are fully accommodated at the two plates. Following [40] the results are given for $Kn_0 = [0.4, 4, 40]$ in one mixture and $Kn_0 = [0.1, 1, 10]$ in the second one with $C_0 = [0.1/1.1, 0.5, 10/11]$ in both mixtures. In order to properly compare the results, the heat fluxes and the Knudsen numbers in [40] are multiplied by the factors $\sqrt{2m_0/m_2}(1-\beta)^{3/2}$ and $(d_2/d_1)^2$ respectively. The relative error between the heat fluxes, defined as $\Delta = 100 \times |q_{BE} - q_{Kosuge}|/q_{BE}$, is also tabulated. It is seen that the heat fluxes agree to at least two significant figures with ±1 in the second figure, with the heat fluxes of the Kosuge model being always lower than the Boltzmann ones. As expected the relative error is increased as the Knudsen number is decreased staying always however less than 4.5%.

In Table 2 the comparison is performed for the mole fractions $C(y)$ at the hot $(y=0)$ and cold $(y=1)$ walls for the virtual HS gas mixture with $m_2/m_1 = 4$, $d_2/d_1 = 2$ and the same reference parameters as in Table 1. It is seen that the agreement remains very good with the maximum percentage deviation between the two approaches being smaller than 1.5%. The mole fractions obtained by the Kosuge model compared to the corresponding Boltzmann ones are always slightly lower at the hot plate and slightly higher at the cold plate. Furthermore, for the same virtual HS gas mixture the comparison is extended to the temperature distributions $\tau(y)$ plotted in Fig. 1. As it seen for all three Knudsen numbers representing all flow regimes and for both mole fractions there is an excellent agreement between the Kosuge model and the Boltzmann equation temperature distributions.

Next, a comparison between the total heat fluxes obtained by the Kosuge model and the DSMC method [41] is performed. Following [41] the comparison refers to He-Ar, with HS molecules, for temperature ratios $T_H/T_C = 1.22$ and $T_H/T_C = 7$, which correspond to weak and strong non-equilibrium heat transfer setups

Table 1
Comparison between the dimensionless total heat flux q obtained by the Kosuge model and the Boltzmann Equation (BE) [40] for two virtual HS gas mixtures with $T_H/T_C = 2$ and for various reference Knudsen numbers Kn_0 and mole fractions C_0.

C_0	Kn_0	$d_2/d_1 = 2$, $m_2/m_1 = 4$			C_0	Kn_0	$d_2/d_1 = 1$, $m_2/m_1 = 2$		
		Kosuge	BE [40]	Δ (%)			Kosuge	BE [40]	Δ (%)
$\frac{0.1}{1.1}$	40	5.14(−1)	5.15(−1)	0.19	$\frac{0.1}{1.1}$	10	4.93(−1)	4.93(−1)	0.00
	4	4.00(−1)	4.06(−1)	1.48		1	3.78(−1)	3.83(−1)	1.31
	0.4	1.48(−1)	1.54(−1)	3.90		0.1	1.34(−1)	1.38(−1)	2.90
$\frac{1}{2}$	40	5.87(−1)	5.88(−1)	0.17	$\frac{1}{2}$	10	5.08(−1)	5.09(−1)	0.20
	4	4.88(−1)	4.95(−1)	1.41		1	3.86(−1)	3.93(−1)	1.78
	0.4	2.15(−1)	2.25(−1)	4.44		0.1	1.35(−1)	1.39(−1)	2.88
$\frac{10}{11}$	40	5.40(−1)	5.40(−1)	0.00	$\frac{10}{11}$	10	4.94(−1)	4.95(−1)	0.20
	4	4.84(−1)	4.88(−1)	0.82		1	3.79(−1)	3.85(−1)	1.56
	0.4	2.77(−1)	2.86(−1)	3.15		0.1	1.35(−1)	1.39(−1)	2.88

Table 2
Comparison between the mole fraction C at the hot and cold plates obtained by the Kosuge model and the Boltzmann Equation (BE) [40] for a virtual HS gas mixture ($d_2/d_1 = 2$, $m_2/m_1 = 4$) with $T_H/T_C = 2$ and for various reference Knudsen numbers Kn_0 and mole fractions C_0.

C_0	Kn_0	Hot plate ($y = 0$)			Cold plate ($y = 1$)		
		Kosuge	BE [40]	Δ (%)	Kosuge	BE [40]	Δ (%)
$\frac{0.1}{1.1}$	40	9.17(−2)	9.22(−2)	0.54	9.01(−2)	8.96(−2)	0.56
	4	9.37(−2)	9.49(−2)	1.26	8.81(−2)	8.69(−2)	1.38
	0.4	9.85(−2)	1.00(−2)	1.50	8.31(−2)	8.18(−2)	1.59
$\frac{1}{2}$	40	5.02(−1)	5.04(−1)	0.40	4.98(−1)	4.95(−1)	0.61
	4	5.10(−1)	5.14(−1)	0.78	4.90(−1)	4.85(−1)	1.03
	0.4	5.30(−1)	5.34(−1)	0.75	4.70(−1)	4.63(−1)	1.51
$\frac{10}{11}$	40	9.10(−1)	9.11(−1)	0.11	9.08(−1)	9.07(−1)	0.11
	4	9.13(−1)	9.15(−1)	0.22	9.05(−1)	9.03(−1)	0.22
	0.4	9.23(−1)	9.24(−1)	0.11	8.93(−1)	8.91(−1)	0.22

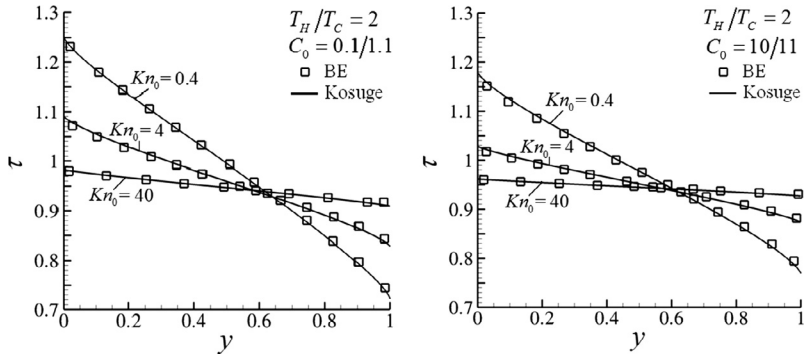

Fig. 1. Comparison between the dimensionless temperature distributions $\tau(y)$ obtained by the Kosuge model and the Boltzmann equation [40] for a HS gas mixture ($d_2/d_1 = 2$, $m_2/m_1 = 4$) with $T_H/T_C = 2$ and for various reference Knudsen numbers Kn_0 and mole fractions C_0.

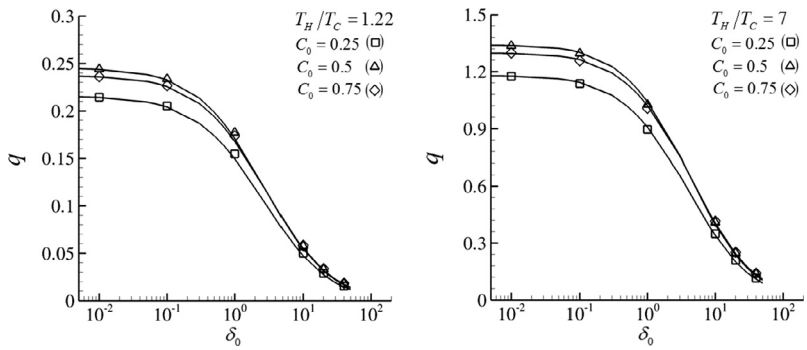

Fig. 2. Comparison between the dimensionless total heat flux q obtained by the Kosuge model (lines) and the DSMC method (symbols) [41] for He-Ar with HS molecules and various reference mole fractions C_0 in terms of the reference rarefaction parameter δ_0 at $T_H/T_C = 1.22$ and $T_H/T_C = 7$.

respectively. Pure diffuse reflection is considered at the two plates. To have a complete view of the comparison in terms of the gas rarefaction, the comparison is presented in graphical form. In Fig. 2, the total heat fluxes obtained by the two approaches are plotted versus the reference gas rarefaction parameter δ_0 for $C_0 = [0.25, 0.5, 0.75]$. The corresponding relative errors, defined as $\Delta = 100 \times |q_{DSMC} - q_{Kosuge}|/q_{DSMC}$, are plotted in Fig. 3. The reference rarefaction parameter δ_0 in [41] is linked to the present reference Knudsen number via

$$Kn_0 = \frac{\sqrt{m_0 k T_0}}{2\pi d_1^2 \mu_0} \frac{1}{\delta_0}, \tag{19}$$

where $d_1 = 0.2173$ nm is the diameter of the He molecule, $\mu_0 = \mu(T_0, C_0)$ is the reference viscosity, obtained from Table 1 in [41] at reference C_0 and $T_0 = 300$ K. In order to properly perform the comparison the DSMC heat fluxes in [41] are multiplied by $\sqrt{8}\beta$. As it is seen, also in this case, where the molecular mass ratio is large ($m_{Ar}/m_{He} \approx 10$), there is good agreement between the results. More specifically, as expected, at $\delta_0 = 0$ the heat fluxes of the two approaches actually coincide, while as δ_0 is increased the relative deviation between the results is monotonically increased up to about $\delta_0 = 20$ and then, as δ_0 is further increased the relative deviation stabilizes around a constant value having a maximum about 5%. The heat fluxes of the Kosuge model are always lower than the corresponding DSMC ones. It is important to note that the agreement between the Kosuge model and the DSMC method is very good not only in the case of small ($T_H/T_C = 1.22$) but also in the case of large ($T_H/T_C = 7$) temperature difference. Additionally, it is noted that the analytical solutions in the free molecular and hydrodynamic limits reported in [41] are fully recovered by the Kosuge model.

Concluding the validation of the results of the Kosuge model a comparison with the Chapman-Enskog solutions [57] for the thermal conductivity and the thermal-diffusion ratio is performed. As it is well-known the Chapman-Enskog solutions of the Boltzmann equation provide a basis for the computation of transport coefficients for single gases and gas mixtures assuming small deviations from the Maxwell–Boltzmann distribution function. In Fig. 4, the thermal conductivities λ_0 (at reference temperature T_0 and mole fraction C_0) of He-Ne and He-Xe with HS molecules are plotted versus the reference temperature T_0 for the Kosuge model and the Chapman-Enskog solutions of the first and seventieth order. The kinetic thermal conductivities have been obtained for $C_0 = [0.2, 0.5, 0.7]$ assuming a small reference Knudsen number ($Kn_0 = 0.015$) and a small temperature ratio between the plates ($T_H/T_C = 1.1$). In these conditions the Chapman-Enskog theory applies well around $y = 0.5$ (far from the Knudsen layers which are adjacent to the walls) and then, in that central region a comparison with the Kosuge kinetic model is feasible using the Fourier law, which in present notation reads as

$$Q = -\lambda \frac{dT}{d\hat{y}}, \tag{20}$$

where λ denotes the thermal conductivity. It is seen in Fig. 4 that the thermal conductivities obtained by the Kosuge model are always in excellent agreement with the first order Chapman-Enskog conductivities of the Boltzmann equation. This is expected since the thermal conductivity of the Kosuge model coincides with that of the original Boltzmann equation at the first approximation [50]. The seventieth order Chapman-Enskog thermal conductivities are always higher and the maximum relative deviation is about 8.5%.

In Fig. 5, the comparison is extended to the thermal-diffusion ratio κ_T, which is defined as [36,57]

$$\frac{dC}{d\hat{y}} = -\frac{\kappa_T}{T} \frac{dT}{d\hat{y}}. \tag{21}$$

In the case of HS molecules the thermal-diffusion ratio depends only on the mole fraction [57]. Thus, in Fig. 5, a comparison between the thermal-diffusion ratios $\kappa_{T,0}$ (at reference mole fraction C_0) obtained by the Kosuge model with the corresponding ones of the Chapman-Enskog analysis of the Boltzmann equation is performed in terms of C_0. As it is seen the kinetic results match very well with those of the Chapman-Enskog analysis for both mixtures (He-Ne and He-Xe) and for all values of C_0.

Based on all above the effectiveness of the Kosuge kinetic model to simulate the present binary gas mixture heat transfer configuration subject to any arbitrary temperature ratio and molecular mass ratio in the whole range of the Knudsen number is demonstrated. The small number of computed negative distributions has a negligible effect on the converged results. The overall efficiency of the implemented computational scheme and the accuracy of the deduced numerical results are verified.

3.2. Macroscopic distributions

The total heat flux, the heat flux of each species, the density, the temperature and the mole fraction distributions of He-Ne, He-Ar and He-Xe with various reference mole fractions C_0 are computed in terms of the temperature ratio T_H/T_C and the reference Knudsen number Kn_0. Partial thermal accommodations of the gas mixture species at the walls are also considered. The hard sphere (HS) [65], Lennard-Jones (LJ) [60] and Realistic Potential (RP) [66] models are introduced. To ensure a comparison on the same basis between the results computed by the three intermolecular potentials, the parameters of each model have been taken so that the deduced values of the thermal conductivity and diffusion

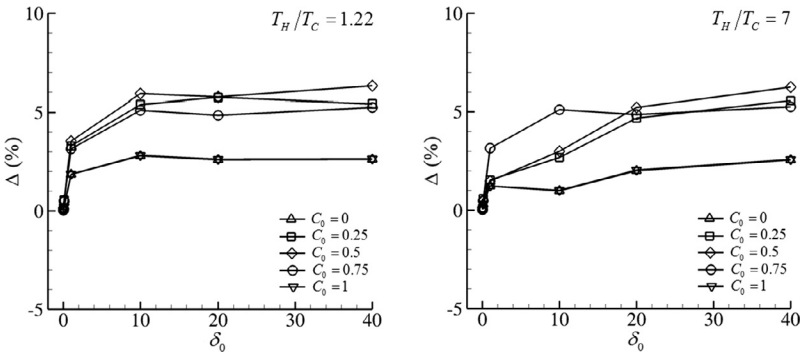

Fig. 3. Relative deviation $\Delta = |q_{DSMC} - q_{Kosuge}|/q_{DSMC}$ between the dimensionless total heat flux q obtained by the Kosuge model and the DSMC method [41] for He-Ar with HS molecules and various reference mole fractions C_0 in terms of the reference rarefaction parameter δ_0 at $T_H/T_C = 1.22$ and $T_H/T_C = 7$.

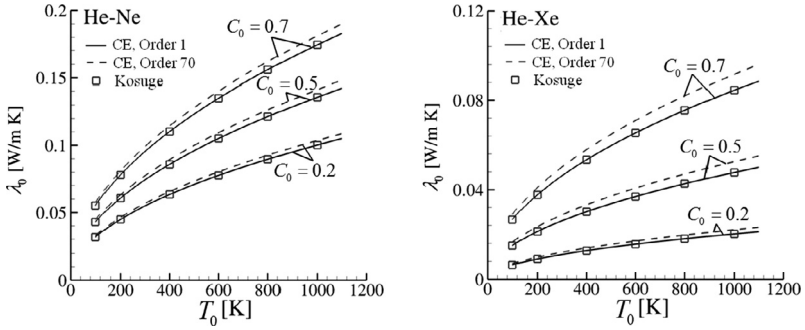

Fig. 4. Comparison between the thermal conductivities λ_0 obtained by the Kosuge model and the first and seventieth order Chapman-Enskog solutions of the Boltzmann equation [57] in terms of the reference temperature T_0 for He-Ne (left) and He-Xe (right) with HS molecules and various mole fractions C_0 at $Kn_0 = 0.015$ and $T_H/T_C = 1.1$.

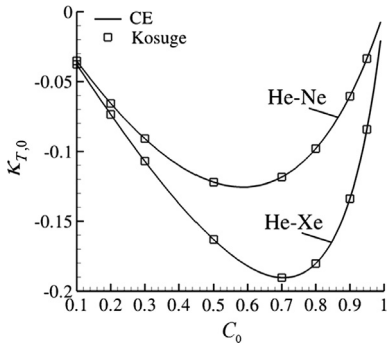

Fig. 5. Comparison between the thermal-diffusion ratios $\kappa_{T,0}$ obtained by the Kosuge model and the Chapman-Enskog solutions of the Boltzmann equation [57] in terms of the reference mole fraction C_0 for He-Ne and He-Xe with HS molecules at $Kn_0 = 0.015$ and $T_H/T_C = 1.1$.

coefficients, at reference temperature $T_0 = 273$ K, are almost the same for all three molecular models (HS, LJ, RP). Obviously, the transport coefficients of the models differ to each other at temperatures $T \neq T_0$, since the temperature dependence of the transport coefficients varies for each intermolecular potential. The introduced parameters are given in Table 3 [59,65,66]. The molecular diameter of He with HS molecules is taken as the reference diameter.

In Tables 4 and 5 the dimensionless total heat fluxes q obtained by the HS model are compared with those of the LJ and RP models for He-Ne and He-Ar respectively, with $T_H/T_C = 1.1$ and $T_H/T_C = 7$, $C_0 = [0.25, 0.5, 0.75]$ and $Kn_0 \in [10^{-2}, 10^2]$. The particles are fully accommodated at the two plates. The results in Tables 4 and 5 include the total heat fluxes of the HS model, while for the LJ and RP models the deviations of their heat fluxes with respect to the corresponding ones of the HS model are tabulated. The deviations are defined as $[100 \times (q^i - q^{HS})/q^{HS}]$, with $i =$ LJ or $i =$ RP for the Lennard-Jones and Realistic Potential respectively. Tabulating the results in that form facilitates the comparison between the models, while the values of the heat fluxes for the LJ and RP models are readily deduced. As it is seen, the discrepancies between the corresponding heat fluxes of the three potentials for both mixtures are negligible in the free molecular regime ($Kn_0 \geqslant 10$) and then, as the Knudsen number is decreased they are gradually increased. The deviations, with regard to the temperature ratio, are larger for $T_H/T_C = 1.1$ compared to the corresponding ones for $T_H/T_C = 7$ and with regard to the mixture composition they are increased as the molecular mass ratio is increased. The largest deviations between the HS and the other two models are for He-Ar with $C_0 = 0.5$, at $Kn_0 = 0.01$ and $T_H/T_C = 1.1$, where they reach 13% and 19% for the LJ and the RP models respectively.

Since the heat flux of each species of the mixture varies between the plates it is interesting to analyze their distributions. In Fig. 6, the heat fluxes $q_1(y)$ and $q_2(y)$ are plotted for He-Ne and He-Ar (HS model) and for $T_H/T_C = 7$, $Kn_0 = 0.01$ and $C_0 = [0.25, 0.5, 0.75]$. Always, the heat flux of the light species, $q_1(y)$, is decreased from the hot towards the cold plate (negative slope) and this reduction becomes more rapid at the vicinity of the cold wall. The heat flux of the heavy species, $q_2(y)$, follows the opposite behavior of that of the light species, i.e., it is increased from the hot towards the cold plate (positive slope), as it should, since the total heat flux between the plates remains constant. Corresponding results obtained by the LJ and the RP models demonstrate a close qualitative resemblance with the presented ones by the HS model. Also, it is noted that as the temperature difference between the plates is decreased and as the Knudsen number is increased the partial heat fluxes tend to be independent of y and remain almost constant between the plates.

In Fig. 7 the density $\rho(y)$ and temperature $\tau(y)$ distributions are plotted for He-Ar (HS model) and for typical values of Kn_0, C_0 and T_H/T_C. The behavior of these distributions is similar to the corresponding ones of a single gas, i.e., for the small temperature ratio ($T_H/T_C = 1.1$) they are symmetric about $y = 0.5$, while for the large

Table 3
Parameters of the Hard-Sphere (HS), Lennard-Jones (LJ) and Realistic Potential (RP) intermolecular models for the gases and binary gas mixtures implemented in the present work [65,66].

Species 1–2	Diameter (cm) $[d \times 10^8]$			Energy parameter (K) $[\varepsilon/k]$	
	HS	LJ	RP	LJ	RP
He-He	2.193	2.70	2.610	6.03	10.40
Ne-Ne	2.602	2.80	2.755	35.7	42.00
Ar-Ar	3.659	3.42	3.350	124	141.5
Xe-Xe	4.882	–	3.885	–	274
He-Ne	2.398	2.75	2.691	23.7	19.44
He-Ar	2.926	3.06	3.084	40.2	30.01
He-Xe	3.538	–	3.533	–	29.77

Table 4
The dimensionless total heat fluxes of the HS model along with the deviations of the heat fluxes of the LJ and RP models with respect to the corresponding HS ones, defined as $[100 \times (q^{i} - q^{HS})/q^{HS}]$, i = LJ, RP, for **He-Ne** with various Kn_0, C_0 and T_H/T_C.

$\frac{T_H}{T_C}$	Kn_0	$C_0 = 0.25$			$C_0 = 0.5$			$C_0 = 0.75$		
		q^{HS}	LJ	RP	q^{HS}	LJ	RP	q^{HS}	LJ	RP
1.1	0.01	2.09(−3)	2.2	5.7	2.34(−3)	2.8	6.5	2.62(−3)	2.2	5.1
	0.1	1.67(−2)	1.8	4.5	1.86(−2)	2.3	5.1	2.02(−2)	1.6	3.9
	1	5.81(−2)	6.0(−1)	1.7	6.33(−2)	6.5(−1)	1.7	6.40(−2)	4.1(−1)	1.3
	10	8.33(−2)	4.2(−2)	2.7(−1)	8.96(−2)	3.4(−2)	2.7(−1)	8.77(−2)	1.4(−2)	2.0(−1)
	50	8.77(−2)	3.2(−3)	6.0(−2)	9.40(−2)	5.0(−4)	5.9(−2)	9.16(−2)	−1.4(−3)	4.3(−2)
	100	8.84(−2)	8.5(−4)	3.1(−2)	9.47(−2)	−5.8(−4)	3.0(−2)	9.21(−2)	−1.2(−3)	2.2(−2)
7	0.01	3.26(−2)	1.4	5.9	3.70(−2)	1.6	6.7	4.14(−2)	8.8(−1)	5.1
	0.1	2.51(−1)	8.5(−1)	4.3	2.81(−1)	9.2(−1)	4.7	3.02(−1)	3.7(−1)	3.4
	1	7.46(−1)	3.6(−2)	1.2	8.11(−1)	−4.0(−3)	1.2	8.13(−1)	−1.3(−1)	7.5(−1)
	10	9.81(−1)	−7.7(−2)	1.5(−1)	1.05	−8.2(−2)	1.5(−1)	1.03	−9.1(−2)	6.1(−2)
	50	1.01	−1.2(−2)	4.0(−2)	1.09	−1.2(−2)	3.7(−2)	1.06	−1.4(−2)	1.5(−2)
	100	1.02	−1.1(−4)	2.3(−2)	1.09	−4.0(−4)	2.1(−2)	1.06	−2.4(−3)	9.4(−3)

Table 5
The dimensionless total heat fluxes of the HS model along with the deviations of the heat fluxes of the LJ and RP models with respect to the corresponding HS ones, defined as $[100 \times (q^{i} - q^{HS})/q^{HS}]$, i = LJ, RP, for **He-Ar** for various Kn_0, C_0 and T_H/T_C.

$\frac{T_H}{T_C}$	Kn_0	$C_0 = 0.25$			$C_0 = 0.5$			$C_0 = 0.75$		
		q^{HS}	LJ	RP	q^{HS}	LJ	RP	q^{HS}	LJ	RP
1.1	0.01	1.38(−3)	11	15	1.88(−3)	13	19	2.46(−3)	10	15
	0.1	1.21(−2)	9.3	13	1.61(−2)	11	16	2.00(−2)	8.2	12
	1	5.50(−2)	4.1	5.6	6.73(−2)	4.4	6.0	7.23(−2)	2.8	4.1
	10	9.24(−2)	7.1(−1)	9.9(−1)	1.07(−1)	7.0(−1)	1.0	1.06(−1)	4.2(−1)	6.4(−1)
	50	1.00(−1)	1.6(−1)	2.3(−1)	1.15(−1)	1.5(−1)	2.2(−1)	1.12(−1)	9.2(−2)	1.4(−1)
	100	1.02(−1)	8.1(−2)	1.2(−1)	1.16(−1)	7.8(−2)	1.1(−1)	1.12(−1)	4.6(−2)	7.2(−2)
7	0.01	2.20(−2)	8.3	10	3.05(−2)	9.9	12	4.05(−2)	6.2	9.1
	0.1	1.88(−1)	6.8	8.4	2.54(−1)	7.7	9.9	3.14(−1)	4.4	6.6
	1	7.40(−1)	2.2	3.3	8.99(−1)	2.1	3.4	9.45(−1)	1.1	2.0
	10	1.10	2.9(−1)	5.4(−1)	1.27	2.8(−1)	5.2(−1)	1.25	1.2(−1)	2.7(−1)
	50	1.17	6.2(−2)	1.2(−1)	1.33	5.9(−2)	1.1(−1)	1.29	2.5(−2)	5.4(−2)
	100	1.17	3.9(−2)	6.9(−2)	1.34	3.4(−2)	5.8(−2)	1.30	1.6(−2)	2.8(−2)

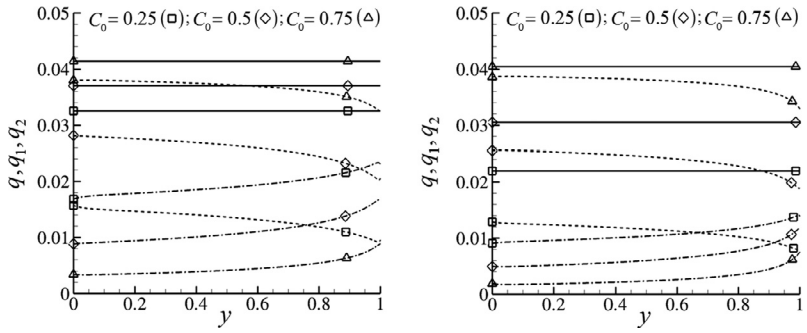

Fig. 6. Distributions of the heat flux of the light $q_1(y)$ (– – – -) and the heavy $q_2(y)$ (— · —) species along with the total heat flux q (———) for He-Ne (left) and He-Ar (right) with HS molecules and for $T_H/T_C = 7$, $Kn_0 = 0.01$ and $C_0 = [0.25, 0.5, 0.75]$.

temperature ratio ($T_H/T_C = 7$) they are not symmetric having a larger temperature jump at the hot wall (compared to that at the cold wall) which is increased as Kn_0 is increased. The effect of C_0 on the density and temperature distributions is, in general, small. It has been also found that the effect of the intermolecular model on the density and temperature distributions is quantitatively small, which is in agreement with corresponding results in [41], where the binary Fourier flow problem has been solved via the DSMC method. To be more specific the relative differences of the number density and temperature for the LJ and RP models compared to the ones of the HS model, defined as $[100 \times (\rho^{HS} - \rho^{i})/\rho^{HS}]$ and $[100 \times (\tau^{HS} - \tau^{i})/\tau^{HS}]$, with i = LJ or i = RP, are less than 1% in the case of $T_H/T_C = 1.1$ and less than 5% in the case of $T_H/T_C = 7$. It is noted that in the case of single gases the corresponding effect of the intermolecular model on the density and temperature distributions has been found to be more significant [67].

On the contrary, the implemented intermolecular model has a more significant effect on the mole fraction distributions. This is demonstrated in Fig. 8, where the mole fraction $C(y)$ is plotted for He-Ar based on the HS, LJ and RP models, with $C_0 = 0.5$, $T_H/T_C = [1.1, 7]$ and $Kn_0 = [10^{-1}, 1, 10^{2}]$. Qualitatively, there is a resemblance between all three models. Quantitatively however, in all cases, the mole fractions distributions based on the LJ and RP models almost coincide, while the ones based on the HS model differ significantly particularly at moderate ($Kn_0 = 1$) and small ($Kn_0 = 0.1$) Knudsen numbers. The mole fraction jumps for the HS model, compared to the other two, are higher. Of course for large values the Knudsen number ($Kn_0 = 10^{2}$) the mole fraction

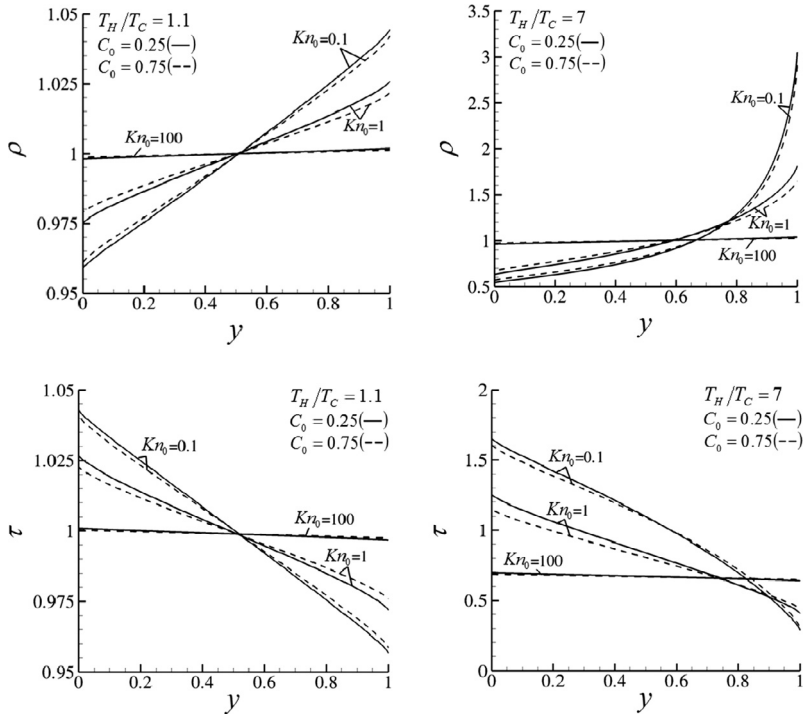

Fig. 7. Distributions of the number density $\rho(y)$ (up) and temperature $\tau(y)$ (down) for He-Ar with HS molecules for $C_0 = 0.25$ (——) and $C_0 = 0.75$ (– – – -) with $T_H/T_C = 1.1$ (left) and $T_H/T_C = 7$ (right) and various values of Kn_0.

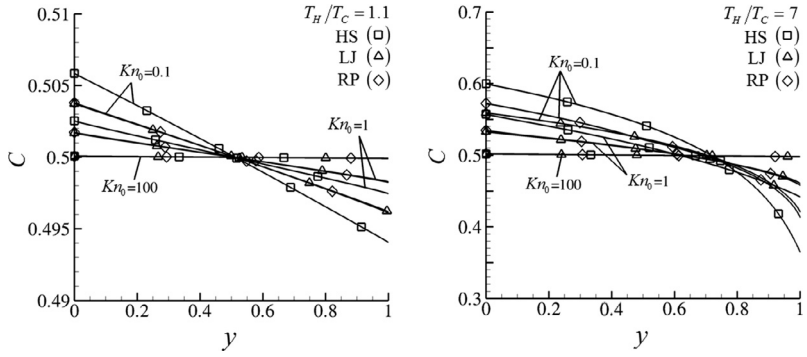

Fig. 8. Distribution of the mole fraction $C(y)$ for He-Ar with HS (□), LJ (△) and RP (◇) potentials for $C_0 = 0.5$ with $T_H/T_C = 1.1$ (left) and $T_H/T_C = 7$ (right) and for various values of Kn_0.

distribution is independent of the intermolecular potential. Overall, the mole fraction distributions behave similarly to the corresponding temperature distributions. This is justified by the fact that according to thermodiffusion, since $m_1 < m_2$ the thermal-diffusion ratio, κ_T is always negative, causing the mole fraction to have a negative slope as it also happens with the temperature distribution. Also, the normalized difference of the mole fraction between the HS and the other two intermolecular potentials (LJ and RP), defined as $[(C^{HS} - C^{i})/(C^{HS}_{y=0} - C^{HS}_{y=1})]$, with $i =$ LJ or $i =$ RP, has been computed in both cases of small and large temperature ratios and it has been found to be of the same order.

Next, the effect of the partial thermal accommodation of the two species at the walls on the heat fluxes for He-Ne and He-Xe is investigated for $Kn_0 = [0.1, 1, 10]$, $C_0 = [0.25, 0.5, 0.75]$ and $T_H/T_C = 1.1$. Only the case of the small temperature difference is considered in order to be closer to experimental works, where typical values for the thermal accommodation coefficients of nobble gases can be found [62–64]. The thermal accommodation coefficient of He has been measured to be smaller than 0.5, while for heavier gases, like Ne and Xe, higher values of the thermal accommodation coefficient have been reported. It is noted that the thermal accommodation coefficient depends not only on the working gas, but also on the physical and mechanical condition of the surface. In Fig. 9, the dimensionless total heat flux of He-Ne and He-Xe based on the HS model in terms of the thermal accommodation of He, α_{He}, is plotted for various values of the thermal accommodation of the heavier gases, α_{Ne} and α_{Xe}. As expected the total heat flux is increased as the gas-surface interaction becomes more diffuse and as the gas mixture becomes less rarefied. With regard to the mole fraction no concrete remarks can be made on the behavior of the heat flux. The presented results for He-Ne and He-Xe may be useful for comparisons with experiments in order to deduce through inverse engineering the accommodation coefficients in the case of binary gas heat transfer.

In order to obtain a more physical understanding of the heat transfer in gas mixtures and to facilitate comparisons with measurements, in Fig. 10, some dimensional heat fluxes Q [W/m^2] are shown in terms of the reference pressure $P_0 = n_0 k T_0$ [Pa] for

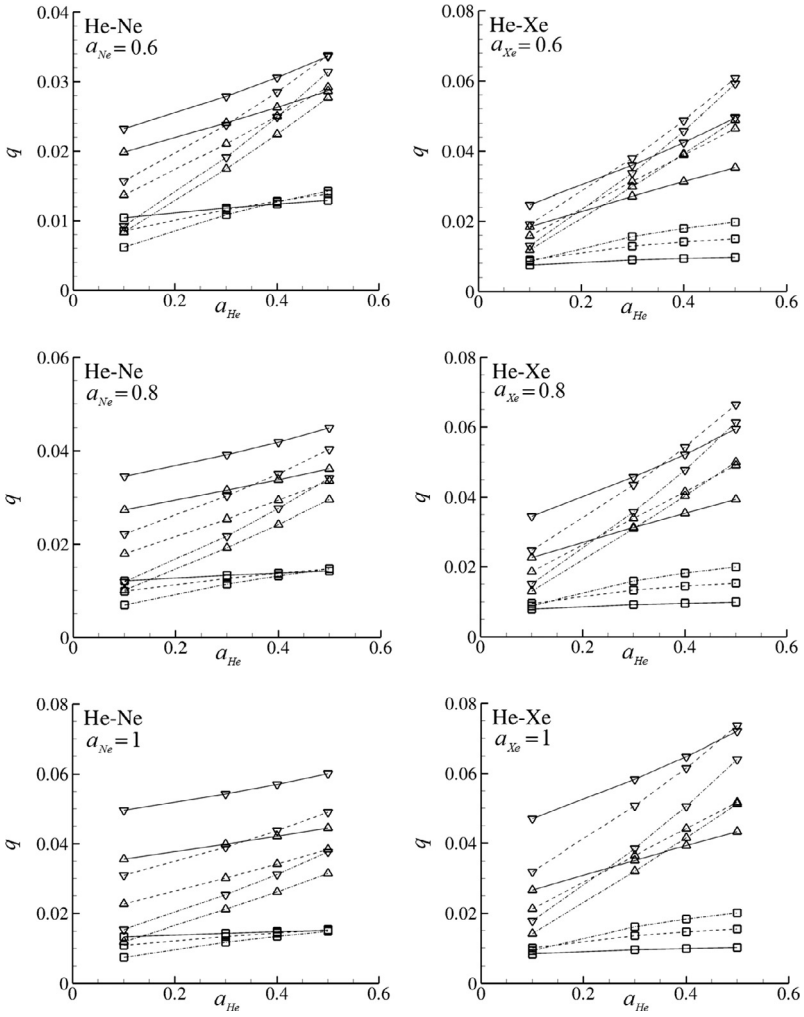

Fig. 9. Dimensionless total heat flux q of He-Ne and He-Xe in terms of the thermal accommodation coefficient of He for various values of the Knudsen number: $Kn_0 = 0.1$ (□), $Kn_0 = 1$ (△), $Kn_0 = 10$ (▽) and for various values of the mole fraction: $C_0 = 0.25$ (——), $C_0 = 0.5$ (– – –), $C_0 = 0.75$ (— · —), with $T_H/T_C = 1.1$.

Ne-Ar and He-Xe with HS molecules and for $0 \leqslant C_0 \leqslant 1$. The reference temperature is set at $T_0 = 573.15$ K and two temperature ratios $T_H/T_C = 1.1$ and 4 are considered. The distance between the parallel plates is set at $L = 0.005$ m. The results for $C_0 = 0$ and $C_0 = 1$ correspond to the heat flux of single gases obtained by the Shakhov kinetic model [52], with the former one referring to the heavy species and the latter one to the light species. It is seen that the heat flux curves with $0 < C_0 < 1$ are bounded from below by the heat flux of the heavy species ($C_0 = 0$) and from above by the heat flux of the light species ($C_0 = 1$). At the same reference pressure P_0, as C_0 is increased, i.e., as the amount of the light species is increased, the gas mixture heat flux is monotonically increased from $Q(C_0 = 0)$ up to $Q(C_0 = 1)$. It is noted that this increment of the heat flux is more intense as the mass ratio m_2/m_1 is increased. Also, as expected, the heat flux is monotonically increased with pressure. More specifically, as in the case of single gases, the binary gas mixture heat flux at highly rarefied atmospheres is proportional to gas pressure, in the transition regime the relation becomes more complex, in the slip regime there is a weak dependence on pressure, reaching finally, in the hydrodynamic regime a constant value.

3.3. Equivalent single gas and effective thermal conductivity concepts

In several practical occasions in order to reduce modeling effort the so-called "equivalent single gas" approach is introduced [58]. In this formulation the binary gas mixture is replaced by a single gas with molecules having the reference molar mass of the mixture, i.e. $m_{eq} = C_0 m_1 + (1 - C_0) m_2$. Then, the analysis is identical to that of the single gas.

In the free molecular limit [41,33] it is readily deduced that the total heat flux Q of the mixture is linked to the total heat flux of the equivalent single gas Q_{eq} as

$$\frac{Q}{Q_{eq}} = C_0 \sqrt{\frac{m_{eq}}{m_1}} + (1 - C_0) \sqrt{\frac{m_{eq}}{m_2}}. \tag{22}$$

Similarly, in the hydrodynamic regime it is found that Q and Q_{eq} are linked according to

$$\frac{Q}{Q_{eq}} = \frac{\mathrm{Pr}_{eq}}{\mathrm{Pr}} = \frac{2}{3\mathrm{Pr}}, \tag{23}$$

where Pr is the Prandtl number of the mixture depending on reference mole fraction C_0 and temperature T_0, while Pr_{eq} is the Prandtl number of the equivalent single gas and it is equal to 2/3. It is noted that relation (23) holds true under the assumptions of small temperature difference between the plates and non-temperature jump at the walls. In the transition regime there is no explicit expression between Q and Q_{eq}.

In Fig. 11, the relative error $100 \times (Q - Q_{eq})/Q$ versus the reference pressure P_0 [Pa] is shown for Ne-Ar and He-Xe (HS model), temperature ratios $T_H/T_C = 1.1$, $T_H/T_C = 4$ and

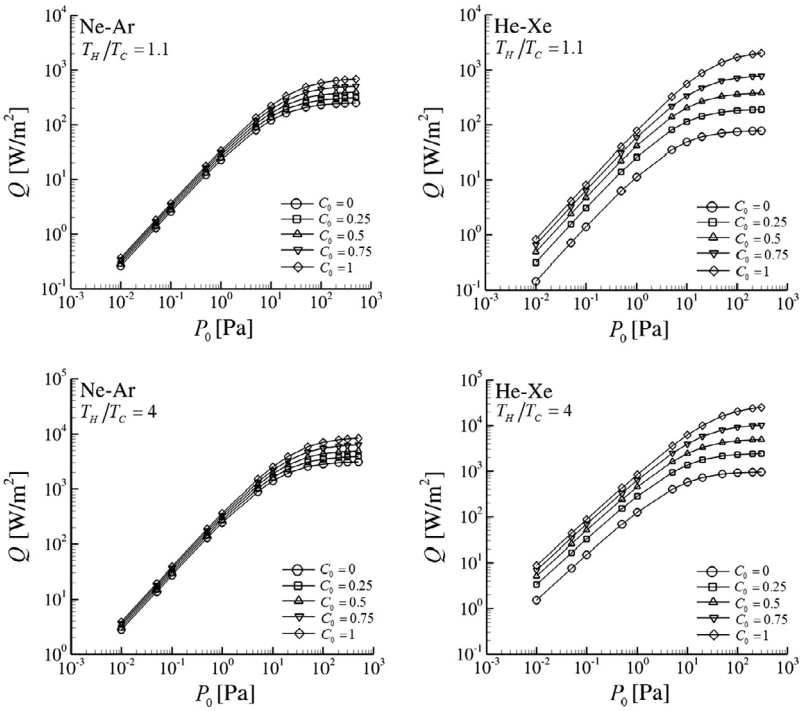

Fig. 10. Dimensional heat flux Q through Ne-Ar and He-Xe enclosed between two plates with distance $L = 0.005$ m for $T_H/T_C = 1.1$ and $T_H/T_C = 4$, with $T_0 = 573.15$, in terms of the reference pressure P_0 for various values of the reference mole fraction C_0.

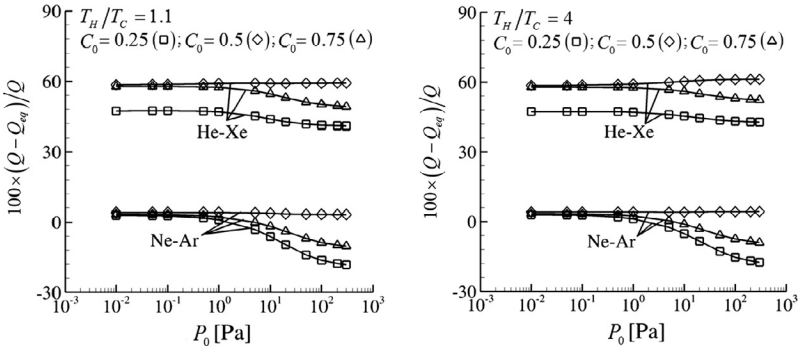

Fig. 11. Relative error $100 \times (Q - Q_{eq})/Q$ introduced by the equivalent single gas approach in terms of reference pressure P_0 [Pa] for Ne-Ar and He-Xe (HS model) with $T_H/T_C = 1.1$ (left) and $T_H/T_C = 4$ (right) and for $C_0 = [0.25, 0.5, 0.75]$.

$C_0 = [0.25, 0.5, 0.75]$. The computed errors at low and high values of the pressure fulfill the analytical expressions (22) and (23) respectively. As shown, for the He-Xe the computed error is always large (more than 40%), which clearly indicates that the equivalent single gas approach cannot be applied. In the case of Ne-Ar the error is small at low pressures and then as pressure is increased for $C_0 = 0.5$ it remains small, while for $C_0 = 0.25$ and 0.75 it is increased. This latter behavior is rather unexpected since as the pressure is increased intermolecular collisions are increased, separation effects are reduced and the gas mixture tends to behave as a single gas [58]. However, as it is indicated by Eq. (23), in the hydrodynamic limit the ratio of the heat fluxes is inversely proportional to the corresponding Prandtl numbers ratio and as it is well known the Plandtl number of a gas mixture depends on the mole fraction and may differ significantly with that of a monatomic gas. Thus the error behavior at large pressure is fully justified and it is seen that even for Ne-Ar having species with molecular masses close to each other the equivalent single gas approach cannot be applied unless C_0 is close to 0.5. Overall, it is concluded that the equivalent single gas approach should not be applied in binary gas mixture heat transfer problems and the problem must be treated by two coupled kinetic equations.

Next, the concept of the effective thermal conductivity in the case of binary gas heat transfer is investigated. It is noted that corresponding analysis for the single monatomic and polyatomic gases has been performed indicating that the effective thermal conductivity approximation may by applied provided that the system Knudsen number is small [21,28]. For the present Fourier flow the effective thermal conductivity is defined as [21]

$$Q = -\lambda_{eff}\frac{dT}{d\hat{y}}, \tag{24}$$

where Q is the total heat flux, $T(\hat{y})$ is the temperature of the mixture computed by the Kosuge model and $\lambda_{eff}(\hat{y})$ is the effective thermal

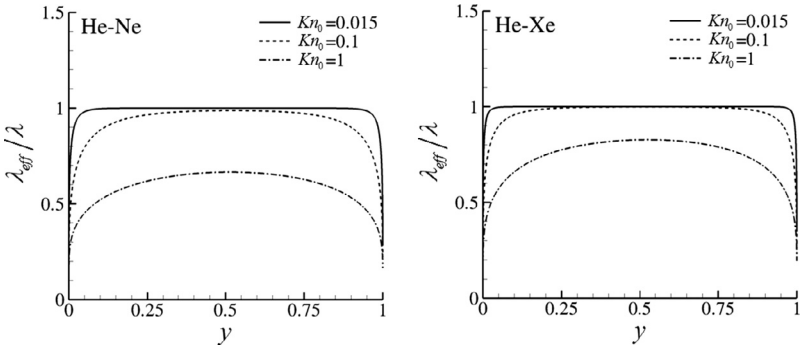

Fig. 12. The ratio λ_{eff}/λ for He-Ne (left) and He-Xe (right) along the distance between the plates for $Kn_0 = [0.015, 0.1, 0.1]$ with $T_H/T_C = 1.1$ and $C_0 = 0.5$.

conductivity which is obtained introducing Q and $T(\hat{y})$ in the Fourier law (24). Next, the ratio λ_{eff}/λ is introduced, where, as mentioned above, $\lambda_{eff} = \lambda_{eff}(\hat{y})$ is the effective thermal conductivity obtained by the Kosuge model and $\lambda = \lambda(\hat{y})$ is the thermal conductivity obtained by the Chapman-Enskog analysis. It is noted that the calculation of the thermal conductivity based on the Chapman-Enskog analysis requires the mole fraction $C(\hat{y})$ which is not known a priori. However, when a small temperature difference is introduced the thermal-diffusion ratio between the plates can be considered constant and then, the mole fraction distribution is computed as [36]

$$C(\hat{y}) = C_0 + \kappa_{T,0}\left(1 - \frac{T(\hat{y})}{T_0}\right), \tag{25}$$

where $\kappa_{T,0} = \kappa_T(T_0, C_0)$ is the thermal diffusion ratio calculated from the Chapman-Enskog analysis at reference T_0 and C_0. Based on the above the thermal conductivity is computed via the first order Chapman-Enskog relations in [57].

In Fig. 12, the ratio λ_{eff}/λ is plotted versus the distance y between the plates for He-Ne and He-Xe (HS model) and $Kn_0 = [0.015, 0.1, 1]$. The temperature ratio is small and equal to $T_H/T_C = 1.1$, with $T_0 = 300$ K, while the mole fraction is taken as $C_0 = 0.5$. When the ratio λ_{eff}/λ is close to one that implies that the Chapman-Enskog analysis is valid and the effective thermal conductivity concept may be applied. As shown, this is true only for $Kn_0 = 0.015$ and $Kn_0 = 0.1$ and also not close to the boundaries, where due to the presence of the Knudsen layers the heat flow is far from local equilibrium. Even for $Kn_0 = 0.015$ the ratio λ_{eff}/λ is rapidly decreased adjacent to the plates. For $Kn_0 = 1$, the atmosphere becomes more rarefied and the Chapman-Enskog solution up to the first order is not valid throughout the domain. Comparing the corresponding results between the He-Ne and He-Xe gas mixtures it is seen that in the latter case, where the molecular mass ratio m_2/m_1 is increased, the deviations from the hydrodynamic behavior are reduced. This is contributed to the fact the heavier particles, compared to the lighter ones, are characterized by smaller mean free paths and therefore the flow is closer to the hydrodynamic regime. Overall, the effective thermal conductivity concept may be applied in binary heat flow setups provided that the system Knudsen number remains adequately small. It is noted that the computational results in Fig. 12, which have been obtained based on kinetic theory, may be implemented in comparisons with results of analytical expressions for the effective thermal conductivity, which are occasionally derived subject to various conditions and assumptions, in order to justify the validity and to determine the applicability range of the closed form expressions. Such expressions are common in single gases mainly for the effective shear viscosity [68,69].

4. Concluding remarks

The problem of heat transfer through rarefied binary gas mixtures confined between two parallel plates maintained at different temperatures has been solved based on the Kosuge kinetic model. The calculations have been carried out for virtual and real mixtures with arbitrary temperature ratio T_H/T_C, over a wide range of the reference Knudsen number Kn_0 and mole fraction C_0. The results obtained by the kinetic model have been compared to corresponding ones obtained by the Boltzmann equation, the DSMC method and the Chapman-Enskog solutions. The Kosuge model has been proven to be computationally efficient providing accurate results even in strongly non-equilibrium heat flow setups.

Furthermore, three intermolecular models, namely the hard sphere (HS), the Lennard Jones (LJ) and the Realistic Potential (RP) models have been implemented in He-Ne and He-Ar. For $Kn_0 \leqslant 1$ the heat fluxes of the HS model vary significantly with the ones of the other two models. Also, the applied interaction model has a significant effect on the mole fraction distribution between the plates, while this effect is not present in the density and temperature distributions. Concerning the partial heat flux distributions of the light and heavy species it has been found that moving from the hot towards the cold plate the former one is decreasing, while the latter one is increasing with the total heat flux being always constant.

The influence of the thermal accommodation coefficient of the species of He-Ne and He-Xe on the computed heat flux has been also investigated. In addition, for the same mixtures dimensional heat fluxes in terms of the reference pressure have been reported indicating that the heat flux is increased along with pressure reaching in the hydrodynamic limit a constant value. Furthermore, the heat fluxes for $0 < C_0 < 1$ are always bounded from below by the heat flux of the heavy species and from above by the heat flux of the light species. These data may be useful for comparisons with experiments in the case of rarefied binary gas heat transfer.

The equivalent single gas approach has been examined to find out that this concept, despite its effectiveness in binary gas mixture flows, does not suit well in binary gas mixture heat transfer problems, which must be treated by two coupled kinetic equations. Finally, the effective thermal conductivity approximation has been introduced and it has been shown that it can be successfully applied, as in the case of single gases, provided that the system Knudsen number remains adequately small.

As it is well known simulating multidimensional rarefied gas problems based on the DSMC method or on the Boltzmann equation is, in general, computationally time consuming. Therefore, successful implementation of reliable kinetic models in such problems is important. Based on the present good performance of the Kosuge model, even in strongly non-equilibrium conditions, it is planned in the short future to apply this model to more demanding non-isothermal flow configurations including gas adsorption.

Conflict of interest

The authors declared that there is no conflict of interest.

Appendix A. Expressions of L_α, Z_α and R_α

The expressions for L_α and Z_α, with $\alpha = 1,2$ and $\beta \neq \alpha$ are given by:

$$L_\alpha = \frac{\rho_\alpha R_\alpha}{2\sqrt{\tau}} + \frac{\sqrt{m_\alpha}}{\sqrt{2m_0}\tau} c_y \Psi_\alpha^{(1)} + \frac{1}{4\tau^{3/2}}\left(\frac{m_\alpha}{m_0}c_y^2 - \tau\right)\Psi_\alpha^{(2)} + \frac{m_\alpha}{m_0}\frac{1}{4\tau^{3/2}}c_y^2\Psi_\alpha^{(3)} + \frac{1}{4\sqrt{\tau}}\left(\Psi_\alpha^{(4)} + \Psi_\alpha^{(5)}\right) + \frac{\sqrt{m_\alpha}}{5\sqrt{2m_0}\tau^2}\left(\frac{m_\alpha}{m_0}c_y^2 - 3\tau\right)c_y\Psi_\alpha^{(6)}, \tag{A.1}$$

$$Z_\alpha = \left(\frac{\rho_\alpha R_\alpha \sqrt{\tau} m_0}{\sqrt{m_1 m_\alpha}}\right) + \sqrt{\frac{2m_0}{m_1}}c_y\Psi_\alpha^{(1)} + \frac{m_0}{2\sqrt{m_1 m_\alpha}\tau}\left(\tau + \frac{m_a}{m_0}c_y^2\right)\Psi_\alpha^{(2)} + \frac{\sqrt{m_\alpha}}{2\sqrt{m_1}\tau}c_y^2\Psi_\alpha^{(3)} + \frac{m_0\sqrt{\tau}}{\sqrt{m_1 m_\alpha}}(\Psi_\alpha^{(4)} + \Psi_\alpha^{(5)}) - \frac{1}{5\tau}\sqrt{\frac{2m_0}{m_1}}\left(\tau - \frac{m_\alpha}{m_0}c_y^2\right)c_y\Psi_\alpha^{(6)}. \tag{A.2}$$

Here the dimensionless quantities $\Psi_\alpha^{(i)}$ $(i = 1,2,\ldots,6)$ are obtained as

$$\Psi_\alpha^{(1)} = \left[\frac{5}{2}\left(\frac{D^{(\beta)}B^{(\alpha)}\sqrt{m_\alpha}}{\sqrt{m_\beta}} - D^{(\alpha)}B^{(\beta)}\right) + \frac{D^{(\beta)}C_{yy}^{(\alpha)}\sqrt{m_\alpha}}{\sqrt{m_\beta}} - D^{(\alpha)}C_{yy}^{(\beta)}\right]\tilde{Y}_{\beta\alpha}^{(1)} + \left(\frac{m_\alpha^2\rho_\alpha D^{(\beta)}}{m_2^{3/2}m_1^{1/2}} - \frac{m_1\rho_\beta D^{(\alpha)}}{m_\alpha}\right)\tilde{v}_{\beta\alpha}^{(2)}, \tag{A.3}$$

$$\Psi_\alpha^{(2)} = \frac{4}{3}\frac{m_\beta - m_\alpha}{m_\beta + m_\alpha}\left[\frac{\tilde{v}_{\beta\alpha}^{(2)}m_\alpha}{2m_2}\left(\frac{15}{2}B^{(\alpha)}B^{(\beta)} + C_{xx}^{(\alpha)}C_{xx}^{(\beta)} + C_{yy}^{(\alpha)}C_{yy}^{(\beta)} + C_{zz}^{(\alpha)}C_{zz}^{(\beta)}\right) - \frac{3D^{(\alpha)}D^{(\beta)}\sqrt{m_\alpha}}{\sqrt{m_\beta}}\tilde{Y}_{\beta\alpha}^{(1)}\right] + R_\alpha B^{(\alpha)} + \frac{2m_\alpha\tilde{v}_{\beta\alpha}^{(1)}}{m_1 + m_2}(\rho_\alpha B^{(\beta)} - \rho_\beta B^{(\alpha)}), \tag{A.4}$$

$$\Psi_\alpha^{(3)} = \rho_\alpha C_{yy}^{(\alpha)}(\tilde{v}_{\alpha\alpha}^{(4)} - \tilde{v}_{\alpha\alpha}^{(3)}) + B^{(\alpha)}C_{yy}^{(\alpha)}(\tilde{Y}_{\alpha\alpha}^{(5)} + \tilde{Y}_{\alpha\alpha}^{(6)}) + \left(\frac{2C_{yy}^{(\alpha)}C_{yy}^{(\alpha)} - C_{xx}^{(\alpha)}C_{xx}^{(\alpha)} - C_{zz}^{(\alpha)}C_{zz}^{(\alpha)}}{3}\right)\tilde{Y}_{\alpha\alpha}^{(7)} + R_\alpha C_{yy}^{(\alpha)} + \frac{2D^{(\alpha)}D^{(\alpha)}}{3}\tilde{Y}_{\alpha\alpha}^{(8)} - \tilde{v}_{\beta\alpha}^{(3)}\rho_\beta C_{yy}^{(\alpha)} + \tilde{v}_{\beta\alpha}^{(4)}\rho_\alpha C_{yy}^{(\beta)} + B^{(\beta)}C_{yy}^{(\alpha)}\tilde{Y}_{\beta\alpha}^{(5)} + B^{(\alpha)}C_{yy}^{(\beta)}\tilde{Y}_{\beta\alpha}^{(6)} + \left(\frac{2C_{yy}^{(\alpha)}C_{yy}^{(\beta)} - C_{xx}^{(\alpha)}C_{xx}^{(\beta)} - C_{zz}^{(\alpha)}C_{zz}^{(\beta)}}{3}\right)\tilde{Y}_{\beta\alpha}^{(7)} + \frac{2D^{(\alpha)}D^{(\beta)}\tilde{Y}_{\beta\alpha}^{(8)}\sqrt{m_\alpha}}{3\sqrt{m_\beta}}, \tag{A.5}$$

$$\Psi_\alpha^{(4)} = \rho_\alpha C_{xx}^{(\alpha)}(\tilde{v}_{\alpha\alpha}^{(4)} - \tilde{v}_{\alpha\alpha}^{(3)}) + B^{(\alpha)}C_{xx}^{(\alpha)}(\tilde{Y}_{\alpha\alpha}^{(5)} + \tilde{Y}_{\alpha\alpha}^{(6)}) + \left(\frac{2C_{xx}^{(\alpha)}C_{xx}^{(\alpha)} - C_{yy}^{(\alpha)}C_{yy}^{(\alpha)} - C_{zz}^{(\alpha)}C_{zz}^{(\alpha)}}{3}\right)\tilde{Y}_{\alpha\alpha}^{(7)} + R_\alpha C_{xx}^{(\alpha)} - \frac{D^{(\alpha)}D^{(\alpha)}}{3}\tilde{Y}_{\alpha\alpha}^{(8)} - \tilde{v}_{\beta\alpha}^{(3)}\rho_\beta C_{xx}^{(\alpha)} + \tilde{v}_{\beta\alpha}^{(4)}\rho_\alpha C_{xx}^{(\beta)} + B^{(\beta)}C_{xx}^{(\alpha)}\tilde{Y}_{\beta\alpha}^{(5)} + B^{(\alpha)}C_{xx}^{(\beta)}\tilde{Y}_{\beta\alpha}^{(6)} + \left(\frac{2C_{xx}^{(\alpha)}C_{xx}^{(\beta)} - C_{yy}^{(\alpha)}C_{yy}^{(\beta)} - C_{zz}^{(\alpha)}C_{zz}^{(\beta)}}{3}\right)\tilde{Y}_{\beta\alpha}^{(7)} - \frac{D^{(\alpha)}D^{(\beta)}\tilde{Y}_{\beta\alpha}^{(8)}\sqrt{m_\alpha}}{3\sqrt{m_\beta}}, \tag{A.6}$$

$$\Psi_\alpha^{(5)} = \rho_\alpha C_{zz}^{(\alpha)}(\tilde{v}_{\alpha\alpha}^{(4)} - \tilde{v}_{\alpha\alpha}^{(3)}) + B^{(\alpha)}C_{zz}^{(\alpha)}(\tilde{Y}_{\alpha\alpha}^{(5)} + \tilde{Y}_{\alpha\alpha}^{(6)}) + \left(\frac{2C_{zz}^{(\alpha)}C_{zz}^{(\alpha)} - C_{xx}^{(\alpha)}C_{xx}^{(\alpha)} - C_{yy}^{(\alpha)}C_{yy}^{(\alpha)}}{3}\right)\tilde{Y}_{\alpha\alpha}^{(7)} + R_\alpha C_{zz}^{(\alpha)} - \frac{D^{(\alpha)}D^{(\alpha)}}{3}\tilde{Y}_{\alpha\alpha}^{(8)} - \tilde{v}_{\beta\alpha}^{(3)}\rho_\beta C_{zz}^{(\alpha)} + \tilde{v}_{\beta\alpha}^{(4)}\rho_\alpha C_{zz}^{(\beta)} + B^{(\beta)}C_{zz}^{(\alpha)}\tilde{Y}_{\beta\alpha}^{(5)} + B^{(\alpha)}C_{zz}^{(\beta)}\tilde{Y}_{\beta\alpha}^{(6)} + \left(\frac{2C_{zz}^{(\alpha)}C_{zz}^{(\beta)} - C_{xx}^{(\alpha)}C_{xx}^{(\beta)} - C_{yy}^{(\alpha)}C_{yy}^{(\beta)}}{3}\right)\tilde{Y}_{\beta\alpha}^{(7)} - \frac{D^{(\alpha)}D^{(\beta)}\tilde{Y}_{\beta\alpha}^{(8)}\sqrt{m_\alpha}}{3\sqrt{m_\beta}}, \tag{A.7}$$

$$\Psi_\alpha^{(6)} = R_\alpha D^{(\alpha)} + \rho_\alpha D^{(\alpha)}(\tilde{v}_{\alpha\alpha}^{(6)} - \tilde{v}_{\alpha\alpha}^{(5)}) + B^{(\alpha)}D^{(\alpha)}(\tilde{Y}_{\alpha\alpha}^{(13)} + \tilde{Y}_{\alpha\alpha}^{(14)}) + C_{yy}^{(\alpha)}D^{(\alpha)}(\tilde{Y}_{\alpha\alpha}^{(15)} + \tilde{Y}_{\alpha\alpha}^{(16)}) - \tilde{v}_{\beta\alpha}^{(5)}\rho_\beta D^{(\alpha)} + \rho_\alpha D^{(\beta)}\frac{\tilde{v}_{\beta\alpha}^{(6)}\sqrt{m_\alpha}}{\sqrt{m_\beta}} + B^{(\beta)}D^{(\alpha)}\tilde{Y}_{\beta\alpha}^{(13)} + \frac{B^{(\alpha)}D^{(\beta)}\tilde{Y}_{\beta\alpha}^{(14)}\sqrt{m_\alpha}}{\sqrt{m_\beta}} + C_{yy}^{(\beta)}D^{(\alpha)}\tilde{Y}_{\beta\alpha}^{(15)} + \frac{C_{yy}^{(\alpha)}D^{(\beta)}\tilde{Y}_{\beta\alpha}^{(16)}\sqrt{m_\alpha}}{\sqrt{m_\beta}}, \tag{A.8}$$

where $B^{(\alpha)}$, $D^{(\alpha)}$, $C_{xx}^{(\alpha)}$, $C_{yy}^{(\alpha)}$, $C_{zz}^{(\alpha)}$ are given as function of the dimensionless macroscopic quantities according to

$$B^{(\alpha)} = \frac{\rho_\alpha}{\tau}(\tau_\alpha - \tau), \quad D^{(\alpha)} = \frac{\sqrt{m_\alpha}}{\sqrt{2m_0}}\frac{q_\alpha}{\tau^{3/2}},$$
$$C_{xx}^{(\alpha)} = \frac{1}{3\tau}(2p_{\alpha xx} - p_{\alpha yy} - p_{\alpha zz}), \quad C_{yy}^{(\alpha)} = \frac{1}{3\tau}(2p_{\alpha yy} - p_{\alpha xx} - p_{\alpha zz})$$
$$C_{zz}^{(\alpha)} = \frac{1}{3\tau}(2p_{\alpha zz} - p_{\alpha xx} - p_{\alpha yy}). \tag{A.9}$$

Introducing the dimensionless quantities of Eq. (10) into Eq. (7), the quantities R_α appearing in Eq. (11) may be written in the following form:

$$R_1 = \frac{\left[\rho_1\left(\tilde{v}_{11}^{(3)} - \tilde{v}_{11}^{(4)}\right) + \rho_2\tilde{v}_{21}^{(3)}\right]\left[\rho_2\left(\tilde{v}_{22}^{(3)} - \tilde{v}_{22}^{(4)}\right) + \rho_1\tilde{v}_{12}^{(3)}\right] - \rho_1\rho_2\tilde{v}_{21}^{(4)}\tilde{v}_{12}^{(4)}}{\rho_2\left(\tilde{v}_{22}^{(3)} - \tilde{v}_{22}^{(4)} + \tilde{v}_{21}^{(4)}\right) + \rho_1\tilde{v}_{12}^{(3)}} \tag{A.10}$$

$$R_2 = R_1\frac{\rho_2\left(\tilde{v}_{22}^{(3)} - \tilde{v}_{22}^{(4)} + \tilde{v}_{21}^{(4)}\right) + \rho_1\tilde{v}_{12}^{(3)}}{\rho_1\left(\tilde{v}_{11}^{(3)} - \tilde{v}_{11}^{(4)} + \tilde{v}_{12}^{(4)}\right) + \rho_2\tilde{v}_{21}^{(3)}} \tag{A.11}$$

The dimensionless collision frequencies $\tilde{v}_{\beta\alpha}^{(i)}$ $(i = 1,2,\ldots,6)$ and $\tilde{Y}_{\beta\alpha}^{(i)}$ $(i = 1,2,\ldots,16)$ are given with respect to their dimensional values that given in Eqs. (A.2) and (A.3) in [50] as

$$\tilde{v}_{\beta\alpha}^{(i)} = \frac{v_{\beta\alpha}^{(i)}}{d_1^2\sqrt{\frac{kT_0}{m_1}}} \quad (i \neq 2), \quad \tilde{v}_{\beta\alpha}^{(2)} = \frac{v_{\beta\alpha}^{(2)}}{d_1^2\sqrt{m_1 kT_0}}, \quad \tilde{Y}_{\beta\alpha}^{(i)} = \frac{Y_{\beta\alpha}^{(i)}}{d_1^2\sqrt{\frac{kT_0}{m_1}}}, \tag{A.12}$$

where d_1 is the molecular diameter of species 1. It is noted that the dimensional $v_{\beta\alpha}^{(i)}$ and $Y_{\beta\alpha}^{(i)}$ are defined in terms of Chapman-Cowling Ω integrals [50].

In the present work the hard sphere, the Lennard-Jones and the realistic potentials are applied and in each case the corresponding Chapman-Cowling Ω integrals are implemented in the following way: for the hard-sphere molecules they are obtained from Eqs. (10.1.1) and (10.2.1) in [65]; for the Lennard-Jones model they are constructed numerically and they may be found in tabulated form in the Appendix F in [60]; finally, for the realistic potential they are calculated from expressions (B7) and (B8) in [66].

References

[1] D.R. Willis, Heat transfer in a rarefied gas between parallel plates at large temperature ratios, in: J.A. Laurmann (Ed.), Rarefied Gas Dynamics, vol. 1, Academic Press, New York, 1963, pp. 209–225.
[2] K. Frankowski, Z. Alterman, C.L. Pekeris, Heat transport between parallel plates in a rarefied gas of rigid sphere molecules, Phys. Fluids 8 (2) (1965) 245–258.
[3] J.R. Thomas, T.S. Chang, C.E. Siewert, Heat transfer between parallel plates with arbitrary surface accommodation, Phys. Fluids 16 (12) (1973) 2116–2120.
[4] I. Graur, A.P. Polikarpov, Comparison of different kinetic models for the heat transfer problem, Heat Mass Transf. 46 (2) (2009) 237–244.
[5] S. Pantazis, D. Valougeorgis, Non-linear heat transfer through rarefied gases between coaxial cylindrical surfaces at different temperatures, Eur. J. Mech. B/Fluids 29 (2010) 494–509.
[6] L. Lees, C.Y. Liu, Kinetic-theory description of conductive heat transfer from a fine wire, Phys. Fluids 5 (10) (1962) 1137–1148.
[7] C.L. Su, D.R. Willis, Heat conduction in a rarefied gas between concentric cylinders, Phys. Fluids 11 (10) (1968) 2131–2143.
[8] C.L. Su, R.W. Springer, A modified discrete ordinate approach to nonlinear cylindrical heat transfer, Int. J. Heat Mass Transf. 13 (1970) 1611–1621.
[9] F. Sharipov, G. Bertoldo, Heat transfer through a rarefied gas confined between two coaxial cylinders with high radius ratio, J. Vac. Sci. Technol., A 24 (6) (2006) 2087–2093.
[10] J.C. Maxwell, The Scientific Papers of James Clark Maxwell, Cambridge University Press, 1890.
[11] L. Lees, Kinetic theory of description of rarefied gas flow, J. Soc. Ind. Appl. Math. 13 (1) (1965) 278–311.
[12] G.S. Springer, S.F. Wan, Note on the application of a moment method to heat conduction in rarefied gases between concentric spheres, AIAA J 4 (8) (1966) 1441–1443.
[13] Y. Wu, Kinetic theory of thermal molecular flow between coaxial cylinders and concentric spheres, J. Chem. Phys. 52 (3) (1970) 1494–1498.
[14] M.T. Ho, I. Graur, Heat transfer through rarefied gas confined between two concentric spheres, Int. J. Heat Mass Transf. 90 (2015) 58–71.
[15] P.L. Bhatnagar, E.P. Gross, M. Krook, A model for collision processes in gases. I. Small amplitude processes in charged and neutral one-component systems, Phys. Rev. 94 (3) (1953) 511–525.
[16] L.H. Holway, New statistical models for kinetic theory: methods of construction, Phys. Fluids 9 (9) (1966).
[17] E.M. Shakhov, Generalization of the Krook kinetic equation, Fluid Dyn. 3 (95) (1968).
[18] F. Sharipov, Rarefied Gas Dynamics: Fundamentals for Research and Practice, Willey-VCH, Germany, 2016.
[19] G.A. Bird, Molecular Gas Dynamics and the Direct Simulation of Gas Flows, Oxford University Press, Oxford, 1994.
[20] M. Vargas, S. Stefanov, D. Valougeorgis, Heat transfer between coaxial cylinders using various molecular interaction models, in: S. Colin, G.L. Morini, (Eds.), Proceedings on CDROM of 2nd European Conference on Microfluidics (μFlu'10), Toulouse, France, SHF (Publisher), 2010, pp. μFLU2010-155:1-10, ISBN 978-2-906831-85-8.
[21] M.A. Gallis, J.R. Torczynski, D.J. Rader, M. Tij, A. Santos, Normal solutions of the Boltzmann equation for highly nonequilibrium Fourier flow and Couette flow, Phys. Fluids 18 (2006) 017104.
[22] H. Akhlaghi, E. Roohi, S. Stefanov, A new iterative wall heat flux specifying technique in DSMC for heating/cooling simulations of MEMS/NEMS, Int. J. Therm. Sci. 59 (2012) 111–125.
[23] L. Wu, C. White, T.J. Scanlon, J.M. Reese, Y. Zhang, A kinetic model of the Boltzmann equation for non-vibrating polyatomic gases, J. Fluid Mech. 763 (2015) 24–50.
[24] B. Rahimi 1, H. Struchtrup, Macroscopic and kinetic modelling of rarefied polyatomic gases, J. Fluid Mech. 806 (2016) 437–505.
[25] V.A. Rykov, A model kinetic equation for a gas with rotational degrees of freedom, Fluid Dyn. 10 (6) (1975) 956–966.
[26] C. Tantos, D. Valougeorgis, M. Pannuzzo, A. Frezzotti, G.L. Morini, Conductive heat transfer in a rarefied polyatomic gas confined between coaxial cylinders, Int. J. Heat Mass Transf. 79 (2014) 378–389.
[27] C. Tantos, D. Valougeorgis, A. Frezzotti, Conductive heat transfer in rarefied polyatomic gases confined between parallel plates via various kinetic models and the DSMC method, Int. J. Heat Mass Transf. 88 (2015) 636–651.
[28] C. Tantos, G.P. Ghiroldi, D. Valougeorgis, A. Frezzotti, Effect of vibrational degrees of freedom on the heat transfer in polyatomic gases confined between parallel plates, Int. J. Heat Mass Transf. 102 (2016) 162–173.
[29] Y. Sone, Effect of sudden change of wall temperature in rarefied gas, J. Phys. Soc. Jpn. 20 (1965) 222–229.
[30] I. Graur, M.T. Ho, Simulation of the transient heat transfer between two coaxial cylinders, J. Vac. Sci. Technol. A: Vac. Surf. Films 31 (2013) 061603.
[31] A. Tsimpoukis, C. Tantos, D. Valougeorgis, Time-dependent conductive heat transfer in rarefied polyatomic gases confined between parallel plates, J. Phys: Conf. Ser. 785 (2017) 012008.
[32] F.J. McCormack, Construction of linearized kinetic models for gaseous mixtures and molecular gases, Phys. Fluids 16 (1973) 2095–2105.
[33] C. Cercignani, F. Sharipov, Gaseous mixture slit flow at intermediate Knudsen numbers, Phys. Fluids A 4 (6) (1992) 1283–1289.
[34] S. Naris, D. Valougeorgis, F. Sharipov, D. Kalempa, Discrete velocity modelling of gaseous mixture flows in MEMS, Superlattices Microstruct. 35 (2004) 629–643.
[35] S. Naris, D. Valougeorgis, D. Kalempa, F. Sharipov, Flow of gaseous mixtures through rectangular microchannels driven by pressure, temperature and concentration gradients, Phys. Fluids 17 (10) (2005), 100607.1-100607-12.
[36] F. Sharipov, L.M.G. Cumin, D. Kalempa, Heat flux through a binary gaseous mixture over the whole range of the Knudsen number, Physica A 378 (2007) 183–193.
[37] R.D.M. Garcia, C.E. Siewert, The McCormack model for gas mixtures: heat transfer in a plane channel, Phys. Fluids 16 (9) (2004) 3393–3402.
[38] A.Ph. Polikarpov, M.T. Ho, I. Graur, Transient heat transfer in a rarefied binary gas mixture confined between parallel plates due to a sudden small change of wall temperatures, Int. J. Heat Mass Transf. 101 (2016) 1292–1303.
[39] M.T. Ho, L. Wu, I. Graur, Y. Zhang, J.M. Reese, Comparative study of the Boltzmann and McCormack equations for Couette and Fourier flows of binary gaseous mixtures, Int. J. Heat Mass Transf. 96 (2016) 29–41.
[40] S. Kosuge, K. Aoki, S. Takata, Heat transfer in a gas mixture between two parallel plates: finite-difference analysis of the Boltzmann equation, in: T.J. Bartel, M.A. Gallis (Eds.), Rarefied Gas Dynamics, 22nd International Symposium, AIP Conference Proceedings, vol. 585, Melvile, 2001, pp. 289–296.
[41] J.L. Strapasson, F. Sharipov, Ab initio simulation of heat transfer through a mixture of rarefied gases, Int. J. Heat Mass Transf. 71 (2014) 91–97.
[42] M. Vargas, S. Stefanov, V. Roussinov, Transient heat transfer flow through a binary gaseous mixture confined between coaxial cylinders, Int. J. Heat Mass Transf. 59 (2013) 302–315.
[43] E.P. Gross, M. Krook, Model for collision processes in gases: Small-amplitude oscillations of charged two-component systems, Phys. Rev. 102 (1956) 593–604.
[44] L. Sirovich, Kinetic modeling of gas mixtures, Phys. Fluids 5 (1962) 908–918.
[45] B.B. Hamel, Kinetic model for binary gas mixtures, Phys. Fluids 8 (1965) 418–425.
[46] L.H. Holway Jr., New statistical models for kinetic theory: Methods of construction, Phys. Fluids 9 (1966) 1658–1673.
[47] H. Oguchi, A kinetic model for a binary mixture and its application to a shock structure, in: C.L. Brundin (Ed.), Rarefied Gas Dynamics, vol. I, Academic Press, New York, 1967, pp. 745–758.
[48] V. Garzó, A. Santos, J.J. Brey, A kinetic model for a multicomponent gas, Phys. Fluids A 1 (a1) (1989) 380–383.
[49] P. Andries, K. Aoki, B. Perthame, A consistent BGK-type model for gas mixtures, J. Stat. Phys. 106 (2002) 993–1018.
[50] S. Kosuge, Model Boltzmann equation for gas mixtures: Construction and numerical comparison, Eur. J. Mech. B/Fluids (2009) 170–184.
[51] S. Kosuge, H. Mizuno, K. Aoki, Numerical investigation on models of the Boltzmann equation for gas mixtures, in: M.S. Ivanov, A.K. Rebrov (Eds.), Rarefied Gas Dynamics, Siberian Branch of the Russian Academy of Sciences, Novosibirsk, 2007, pp. 286–291.
[52] S. Pantazis, D. Valougeorgis, Heat transfer between parallel plates via kinetic theory in the whole range of the Knudsen number, Paper 407, 5th European Thermal-Sciences Conference, 19-22/5/2008, Eindhoven, Netherlands, 2008.
[53] E.M. Shakhov, V.A. Titarev, Numerical study of the generalized cylindrical Couette flow of rarefied gas, Eur. J. Mech. B/Fluids 28 (1) (2009) 152–169.
[54] S. Pantazis, S. Naris, C. Tantos, D. Valougeorgis, J. Andre, F. Millet, J.P. Perin, Nonlinear vacuum gas flow through a short tube due to to pressure and temperature gradients, Fusion Eng. Des. 88 (2013) 2384–2387.
[55] V.V. Aristov, E.M. Shakhov, V.A. Titarev, S.A. Zabelok, Comparative study for rarefied gas flow into vacuum through a short circular pipe, Vacuum 103 (2014) 5–8.
[56] G. Tatsios, M. Vargas, D. Valougeorgis, S. Stefanov, Non-equilibrium gas flow and heat transfer in a heated square microcavity, Heat Transf. Eng. 37 (13–14) (2016) 1085–1095.
[57] E.L. Tipton, R.V. Tompson, S.K. Loyalka, ChapmanEnskog solutions to arbitrary order in Sonine polynomials III: Diffusion, thermal diffusion, and thermal conductivity in a binary, rigid-sphere, gas mixture, Eur. J. Mech. B/Fluids 28 (2009) 353–386.
[58] D. Valougeorgis, M. Vargas, S. Naris, Analysis and guidelines on gas separation, conductance and equivalent single gas approach for binary gas mixture expansion through a short tube into vacuum, Vacuum 128 (2016) 1–8.
[59] S. Kosuge, S. Takata, Database for flows of binary gas mixtures through a plane microchannel, Eur. J. Mech. B/Fluids 27 (2008) 444–465.
[60] I.N. Ivchenko, S.K. Loyalka, R.V. Thompson Jr., Analytical Methods for Problems of Molecular Transport, Springer, Dordrecht, The Netherlands, 2007.
[61] A. Frezzotti, G.P. Ghiroldi, L. Gibelli, Rarefied gas mixtures flows driven by surface absorption, Vacuum 86 (11) (2012) 1731–1738.
[62] I.N. Larina, V.A. Rykov, Boundary conditions for gases on a body surface, Fluid Dyn. 21 (1986) 795–801.
[63] Y.G. Semyonov, S.F. Borisov, P.E. Suetin, Investigation of heat transfer in rarefied gases over a wide range of Knudsen number, Int. J. Heat Mass Transf. 27 (10) (1984) 1789–1799.
[64] W.M. Trott, J.N. Castaneda, J.R. Torczynski, M.A. Gallis, D.J. Rader, An experimental assembly for precise measurement of thermal accommodation, Rev. Sci. Instrum. 82 (2011) 035120.
[65] S. Chapman, T.G. Cowling, The Mathematical Theory of Non-Uniform Gases, third ed., Cambridge University Press, Cambridge, 1990.

[66] J. Kestin, K. Knierim, E.A. Mason, B. Najafi, S.T. Ro, M. Waldman, Equilibrium and transport properties of the noble gases and their mixture at low densities, J. Phys. Chem. Ref. Data 13 (1984) 229–303.
[67] L. Wu, H. Liu, Y. Zhang, J.M. Reese, Influence of intermolecular potentials on rarefied gas flows: Fast spectral solutions of the Boltzmann equation, Phys. Fluids 27 (2015) 082002.
[68] Z. Guo, C. Zheng, B. Shi, Lattice Boltzmann equation with multiple effective relaxation times for gaseous microscale flow, Phys. Rev. E 77 (2008) 036707.
[69] W. Su, S. Lindsay, H. Liu, L. Wu, Comparative study of the discrete velocity and lattice Boltzmann methods for rarefied gas flows through irregular channels, Phys. Rev. E 96 (2017) 023309.